

# On Area Growth in Sol

Richard Evan Schwartz \*

December 23, 2020

## Abstract

Let Sol be the 3-dimensional solvable Lie group whose underlying space is  $\mathbf{R}^3$  and whose left-invariant Riemannian metric is given by

$$e^{-2z}dx^2 + e^{2z}dy^2 + dz^2.$$

We prove that the sphere of radius  $r$  in Sol has surface area at most  $20\pi e^r$  provided that  $r$  is sufficiently large. This estimate is sharp up to a factor of 10.

## 1 Introduction

Sol is one of the 8 Thurston geometries [Th], the one which uniformizes torus bundles which fiber over the circle with Anosov monodromy. Sol has been studied in various contexts: coarse geometry [EFW], [B]; minimal surfaces [LM] (etc.); its geodesics [G], [T], [K], [BS]; connections to Hamiltonian systems [A], [BT]; and finally virtual reality [CMST]. Our paper [CS] has a more extensive discussion of these many references.

In [CS], Matei Coiculescu and I give an exact characterization of which geodesic segments in Sol are length minimizers, thereby giving a precise description of the cut locus of the identity in Sol. As a consequence, we proved that the metric spheres in Sol are topological spheres, smooth away from 4 singular arcs. We will summarize the characterization in §2 and explain the main ideas in the proof in §4.

---

\*Supported by N.S.F. Grant DMS-1807320

Ian Agol recently pointed out to me that our exact characterization of the cut locus in Sol might help us determine the growth rate in balls in Sol. Eryk Kopczyński pointed out a rather easy calculation that  $V_r \leq Cr^2e^r$  for some constant  $C$ , and this implies that Sol has volume entropy 1. See §2.8. Marc Troyanov recently showed me a preprint with the estimate  $V_r < 8re^r$ . We will get finer information.

To state our main result, we normalize the metric in Sol so that it is:

$$e^{-2z} dx^2 + e^{2z} dy^2 + dz^2. \quad (1)$$

In this metric the planes  $X = 0$  and  $Y = 0$  have sectional curvature  $-1$ . Let  $\mathcal{S}_r$  denote any metric sphere of radius  $r$  in Sol. Let  $A_r$  denote the area of  $\mathcal{S}_r$  with respect to the Riemannian metric in Sol.

**Theorem 1.1**  $A_r < 20\pi e^r$  provided that  $r$  is sufficiently large.

**Remarks:**

(i) Given the 2-to-1 locally-area-decreasing projection from  $\mathcal{S}_r$  onto the hyperbolic disk of radius  $r$ , we have  $A_r > 4\pi(\cosh(r) - 1) \approx 2\pi e^r$ . Thus, our estimate is sharp up to a factor of 10.

(ii) Our analysis does not give an effective estimate on what “sufficiently large” means. However, we notice that all the relevant quantities seem to stabilize pretty quickly: one sees all the phenomena already when looking at a sphere of radius 8 in Sol.

The basic idea of the proof is to bound the projections of the sphere into the coordinate planes. Let  $\Pi_X$  denote the coordinate plane  $X = 0$ . Let  $\eta_X$  denote the projection of Sol into  $\Pi_X$ . Let  $A_{X,r}$  denote the area of  $\eta_X(\mathcal{S}_r)$ . Let  $N_{X,r}$  denote the smallest integer such that the map  $\eta_X : \mathcal{S}_r \rightarrow \Pi_X$  is at most  $N_{X,r}$ -to-1. We make all the same definitions with  $Y$  and  $Z$  in place of  $X$ . We also make a more refined definition for  $Z$ . Let  $\mathcal{S}_{r,k}$  denote the subset where  $\eta_Z$  is  $k$ -to-1, We let  $A_{Z,r,k}$  denote the area of  $\eta_Z(\mathcal{S}_{r,k})$ . In §2.7 we prove the following result.

**Lemma 1.2 (Projection)** For any  $\epsilon > 0$  and any  $\theta \in (0, 1)$  we may take  $r$  sufficiently large so that

$$A_r < \frac{(N_{X,r}A_{X,r} + N_{Y,r}A_{Y,r})}{\theta - \epsilon} + \frac{1}{\sqrt{1 - \theta^2} - \epsilon} \sum_{k=1}^{\infty} kA_{Z,k,r}.$$

**Remark:** A similar result would be true for any surface in Sol which is almost everywhere smooth, but the formula in general would not be quite as good. We use special properties of  $\mathcal{S}_r$  to get the formula above.

We then establish the following *projection estimates*:

1.  $A_{X,r} = A_{Y,r} = 2\pi(\cosh(r) - 1) < \pi e^r$ .
2.  $N_{X,r} = N_{Y,r} = 2$ .
3.  $A_{Z,r} < 16^* e^r$  for sufficiently large  $r$ .
4.  $N_{Z,r} = 4$  for sufficiently large  $r$ .
5.  $A_{Z,k,r} < 0^* e^r$  for  $k = 3, 4$ .

The number  $\zeta^*$  is a number we can make as close as we like to  $\zeta$  by taking  $r$  sufficiently large. Estimates 4 and 5 together combine to say that the projection  $\eta_Z$  is essentially 2-to-1, because the set where it is either 3-to-1 or 4-to-1 has negligible area in comparison to  $e^r$ . When we apply the result in Lemma 1.2 we see that, for  $r$  large,

$$A_r < \min_{\theta \in (0,1)} \left( \frac{4^* \pi}{\theta} + \frac{32^*}{\sqrt{1-\theta^2}} \right) e^r < 20\pi e^r. \quad (2)$$

The minimizer is quite close to  $\theta = 3/5$  and the minimum is about  $60.93e^r$ .

Projection Estimates 1 and 2 are straightforward given our description of the Sol spheres. Projection Estimate 3 relies on an analysis of an ODE studied in [CS] and some easy asymptotic results about elliptic functions. After giving our upper bound we will explain, a bit sketchily, why

$$A_{Z,r} > (2/1^*)e^r$$

once  $r$  is sufficiently large. We do this to point out that our upper bound is fairly tight. When we plug in this smaller estimate into the Projection formula above, we get a bound of about  $7\pi e^r$ . This represents a kind of absolute limit to the strength of our method.

The hard work in the paper involves dealing with Projection Estimate 4, even though the result is clear from the computer plots such as Figure 5.4, involves a careful asymptotic study of the ODE just mentioned. Projection Estimate 5 comes out as a byproduct of our analysis.

This paper is organized as follows.

- In §2 we introduce some preliminary material and in particular recall the Main Theorem from [CS]. We use this result to prove the Projection Lemma, though we also point out that one can prove the Projection Lemma knowing a much softer result about the Sol spheres.
- In §3, we prove Projection Estimates 1 and 2.
- In §4, we give details about the proof of the Main Theorem in [CS]. These details are needed for the proof of Projection Estimates 3 – 5.
- In §5 we give more information about the central ordinary differential equations which arise in [CS].
- In §6 we prove Projection Estimates 3 – 5 modulo the detail that a certain curve in the plane is smooth and regular except at a single cusp. See Figure 5.3. Proving this result, which we call the Embedding Theorem, turns out to be a fight with the OEDs introduced in §5.
- In §7 we prove the Embedding Theorem modulo a detail which we call the Monotonicity Lemma, a statement about the ODE from §4.3.
- in §8-9 we prove the Monotonicity Lemma. This is where all the ODE calculations come in.

I would like to thank Ian Agol, Matei Coiculescu, Justin Holmer, Anton Izosimov, Boris Khesin, Eryk Kopczyński, Mark Levi, Benoit Pausader, Pierre Pansu, and Marc Troyanov for helpful discussions concerning this paper. I would also like to acknowledge the support of the Simons Foundation, in the form of a 2020-21 Simons Sabbatical Fellowship, and also the support of the Institute for Advanced Study, in the form of a 2020-21 membership funded by a grant from the Ambrose Monell Foundation.

## 2 Preliminaries

### 2.1 Basic Properties of Sol

The underlying space for Sol is  $\mathbf{R}^3$ . The metric is:

$$e^{-2z} dx^2 + e^{2z} dy^2 + dz^2. \quad (3)$$

The group law on Sol is

$$(x, y, z) * (a, b, c) = (e^z a + x, e^{-z} b + y, c + z). \quad (4)$$

Left multiplication is an isometry. We identify  $\mathbf{R}^3$  with the Lie algebra of Sol in the obvious way. (See [CS, §2.1] if this does not seem obvious.)

Sol has 3 interesting foliations.

- The XY foliation is by (non-geodesically-embedded) Euclidean planes.
- The XZ foliation is by geodesically embedded hyperbolic planes.
- The YZ foliation is by geodesically embedded hyperbolic planes.

The complement of the union of the two planes  $X = 0$  and  $Y = 0$  is a union of 4 *sectors*. One of the sectors, the *positive sector*, consists of vectors of the form  $(x, y, z)$  with  $x, y > 0$ . The sectors are permuted by the Klein-4 group generated by isometric reflections in the planes  $X = 0$  and  $Y = 0$ . The Riemannian exponential map  $E$  preserves the sectors. Usually, this symmetry will allow us to confine our attention to the positive sector.

**Notation:** For each  $W \in \{X, Y, Z\}$ , the plane  $\Pi_W$  is given by  $W = 0$  and the map  $\eta_W : \text{Sol} \rightarrow \Pi_W$  is the projection onto  $\Pi_W$  obtained by just dropping the  $W$  coordinate. We also let  $\pi_Z$  denote projection onto the  $Z$ -axis. Thus,  $\pi_Z(x, y, z) = z$ .

### 2.2 Properties of the Hyperbolic Slices

We discuss our results for  $\Pi_Y$ . There are analogous results for  $\Pi_X$ . Here is a basic property of the hyperbolic slices in Sol. The map  $F(x, 0, z) = (x, e^z)$  converts the metric in  $\Pi_Y$  to the standard hyperbolic metric in the upper half plane, namely

$$(dx^2 + dy^2)/y^2.$$

**Lemma 2.1** *In  $\Pi_Y$ , the points  $(0, 0, 0)$  and  $(d_r, 0, 0)$  are connected by a geodesic segment of length  $r$  when  $d_r = e^{r/2} - e^{-r/2}$ .*

**Proof:** Here  $d_r = 2 \sinh(r/2)$ . Let  $F$  be the transformation from  $\Pi_Y$  to the standard upper half plane model. We have  $F(0, 0, 0) = (0, 1)$  and  $F(d_r, 0, 0) = (d_r, 1)$ . As is well known, the distance between these points in the standard hyperbolic metric is  $2 \sinh^{-1}(d_r/2) = 2(r/2) = r$ . ♠

**Lemma 2.2** *In  $\Pi_Y$ , the point  $(x, 0, z)$  lies in the disk of radius  $r$  centered at  $(0, 0, 0)$  only if  $|x| \leq (e^r - e^{-r})/2$ .*

**Proof:** We use the transformation  $F$  again. Looking in the standard upper half plane model, the disk we are interested in,  $D_r$ , is centered at  $(0, 1)$  and has radius  $r$ . The two points  $(0, e^{-r})$  and  $(0, e^r)$  lie in the boundary of  $D_r$ . Hence  $D_r$  has Euclidean radius  $(e^r - e^{-r})/2$ . ♠

## 2.3 The Disk Lemma

Here we recall a result from topology. This result will be useful, in §5, when we prove Projection Estimate 4.

**Lemma 2.3 (Disk)** *Let  $\Delta \subset \mathbf{R}^2$  be a disk. Let  $h : \Delta \rightarrow \mathbf{R}^2$  be a map which is a local diffeomorphism on the interior such that  $h(\partial\Delta)$  is a piecewise smooth curve having finitely many self-intersections. Given  $p \in \mathbf{R}^2 - h(\Delta)$ , the number of preimages  $h^{-1}(p)$  equals the unsigned number of times  $h(\partial\Delta)$  winds around  $p$ .*

**Proof:** This is a well-known result. Here we sketch the proof. Without loss of generality, we can assume that  $\Delta$  is the unit disk in  $\mathbf{R}^2$  and  $h(0, 0) \neq p$ . Let  $\Delta_s$  denote the disk of radius  $s$  centered at  $(0, 0)$ . Also, we can assume that  $h$  is orientation preserving in the interior of  $\Delta$ . Let  $f(s)$  denote the number of times  $h(\Delta_s)$  winds around  $p$ . For  $s$  near 0, we have  $f(s) = 0$ . The function  $f$  changes by  $\pm 1$  each time  $\Delta_s$  crosses a point of  $f^{-1}(p)$ . The sign is always the same because  $h$  is orientation preserving. Hence the number of points in  $f^{-1}(p)$  equals  $f(1)$ , up to sign. ♠

## 2.4 Elliptic Functions

Many of the quantities associated to Sol are expressed in terms of elliptic integrals. The complete elliptic functions of the first and second kind are given by

$$\mathcal{K}(m) = \int_0^{\pi/2} \frac{d\theta}{\sqrt{1 - m \sin^2 \theta}}, \quad \mathcal{E}(m) = \int_0^{\pi/2} \sqrt{1 - m \sin^2(\theta)} d\theta. \quad (5)$$

The first integral is defined for  $m \in [0, 1)$  and the second one is defined for  $m \in [0, 1]$ . These functions satisfy the following differential equations. For a proof see any textbook on elliptic functions.

$$\frac{d\mathcal{K}}{dm} = \frac{(m-1)\mathcal{K} + \mathcal{E}}{2m - 2m^2}, \quad \frac{d\mathcal{E}}{dm} = \frac{-\mathcal{K} + \mathcal{E}}{2m}. \quad (6)$$

We will use the following classic identity.

$$\mathcal{K}(m) = \frac{\pi/2}{\text{AGM}(\sqrt{1-m}, 1)}, \quad m \in (0, 1). \quad (7)$$

See [BB] for a proof. We also have

$$\mathcal{E}(1) = 1, \quad \lim_{m \rightarrow 1} \frac{\mathcal{K}(m)}{|\log(1-m)|} = 2. \quad (8)$$

The second equation is much more than we need for the proof of Lemma 8.1 below. We just need to know that  $\mathcal{K}(m)$  grows more slowly than  $1/(1-m)$ .

## 2.5 The Hamiltonian Flow

Let  $G = \text{Sol}$ . Let  $S_1 \subset \mathbf{R}^3$  denote the unit sphere. at the origin in  $G$ . Given a unit speed geodesic  $\gamma$ , the tangent vector  $\gamma'(t)$  is part of a left invariant vector field on  $G$ , and we let  $\gamma^*(t) \in S_1$  be the restriction of this vector field to  $(0, 0, 0)$ . In terms of left multiplication on  $G$ , we have the formula

$$\gamma^*(t) = dL_{\gamma(t)^{-1}}(\gamma'(t)). \quad (9)$$

It turns out that  $\gamma^*$  satisfies the following differential equation.

$$\frac{d\gamma^*(t)}{dt} = \Sigma(\gamma^*(t)), \quad \Sigma(x, y, z) = (+xz, -yz, -x^2 + y^2). \quad (10)$$

This is explained one way in [G] and another way in [CS, §5.1]. (Our formula has a different sign than Grayson's, because our group law correspondingly differs by a sign.) This system in Equation 10 is really just geodesic flow on the unit tangent bundle of Sol, viewed in a left-invariant reference frame.

Let  $F(x, y, z) = xy$ . The flow lines of  $\Sigma$  lie in the level sets of  $F$ , and indeed  $\Sigma$  is the Hamiltonian flow generated by  $F$ . Most of the level sets of  $F$  are closed loops. We call these *loop level sets*. With the exception of the points in the planes  $X = 0$  and  $Y = 0$ , and the points  $(x, y, 0)$  with  $|x| = |y| = \sqrt{2}$ , the remaining points lie in loop level sets.

Each loop level set  $\Theta$  has an associated *period*  $L = L_\Theta$ , which is the time it takes a flowline – i.e., an integral curve – in  $\Theta$  to flow exactly once around. Equation 11 below gives a formula. We can compare  $L$  to the length  $T$  of a geodesic segment  $\gamma$  associated to a flowline that starts at some point of  $\Theta$  and flows for time  $T$ . We call  $\gamma$  *small*, *perfect*, or *large* according as  $T < L$ , or  $T = L$ , or  $T > L$ . In [CS, §5] we prove the following result:

**Theorem 2.4** *Suppose  $(x, y, z) \in S^2$  lies in a loop level set. Let  $\alpha = \sqrt{|xy|}$ . Then the period of the loop level set containing  $(x, y, z)$  is*

$$L_\alpha = \frac{\pi}{\text{AGM}(\alpha, \frac{1}{2}\sqrt{1+2\alpha^2})} = \frac{4}{\sqrt{1+2\alpha^2}} \times \mathcal{K}\left(\frac{1-2\alpha^2}{1+2\alpha^2}\right). \quad (11)$$

The second expression follows from the first, and from Equation 7.

Each vector  $V = (x, y, z)$  simultaneously corresponds to two objects:

- The flowline  $\phi_V$  which starts at  $V/\|V\|$  and goes for time  $\|V\|$ .
- The geodesic segment  $\gamma_V = \{E(tV) \mid t \in [0, 1]\}$ .

Given a vector  $V = (x, y, z)$  we define

$$\mu(V) = \text{AGM}(\sqrt{xy}, \frac{1}{2}\sqrt{(|x| + |y|)^2 + z^2}). \quad (12)$$

We call  $V$  *small*, *perfect*, or *large* according as  $\mu(V)$  is less than, equal to, or greater than  $\pi$ . In view of Equation 11 here is what this means:

- If  $\gamma_V$  lies in the plane  $X = 0$  or  $Y = 0$  then  $V$  is small because  $\mu(V) = 0$ .
- If  $V = (x, y, 0)$  where  $|x| = |y|$  then  $V$  is small, perfect, or large according as  $|x| < \pi$ ,  $|x| = \pi$  or  $|x| \geq \pi$ .
- In all other cases,  $V/\|V\|$  lies in a loop level set, and  $V$  is small, perfect, or large according as  $\mu(V) < \pi$ ,  $\mu(V) = \pi$ , or  $\mu(V) > \pi$ .

## 2.6 The Main Result

Now we recall the main result from [CS].

**Theorem 2.5** *Given any vector  $V$ , the geodesic segment  $\gamma_V$  is a distance minimizing geodesic if and only if  $\mu(V) \leq \pi$ . That is,  $\gamma_V$  is distance minimizing if and only if  $V$  is small or perfect. Moreover, if  $V$  and  $W$  are perfect vectors then  $E(V) = E(W)$  if and only if  $V = (x, y, z)$  and  $W = (x, y, \pm z)$ .*

Theorem 1.1 identifies the cut locus of the identity in Sol with the set of perfect vectors. The Riemannian exponential map  $E$  is a global diffeomorphism on the set of small vectors. Also,  $E$  is generically 2-to-1 on the set of perfect vectors. We will explain this last fact below.

Theorem 1.1 leads to a good description of the Sol metric sphere  $\mathcal{S}_r$  of radius  $r$ . Let  $S_r$  denote the Euclidean sphere of radius  $r$  centered at the origin of  $\mathbf{R}^3$ . Let

$$S'_r = \mu^{-1}[0, \pi] \cap S_r. \quad (13)$$

The space  $S'_r$  is a 4-holed sphere. The boundary  $\partial S'_r$ , a union of 4 loops, is precisely the set of perfect vectors contained in  $S_r$ . Each of these loops is homothetic to one of the loop level sets on the unit sphere  $S^2$ . The Klein-4 symmetry explains why there are 4 such loops.

It follows from the Main Theorem that  $\mathcal{S}_r = E(S'_r)$  and that  $E$  is a diffeomorphism when restricted to  $S'_r - \partial S'_r$ . On  $\partial S'_r$ , the map  $E$  is a 2-to-1 folding map which identifies partner points within each component. Thus, we see that  $\mathcal{S}_r$  is obtained from a 4-holed sphere by gluing together each boundary component (to itself) in a 2-to-1 fashion. This reveals  $\mathcal{S}_r$  to be a topological sphere which is smooth away from the set  $E(\partial S'_r)$ . We also prove that the singular set  $E(\partial S'_r)$  consists of 4 arcs of hyperbolas, all contained in  $\Pi_Z$ .

**The Lunar Principle:** Given a unit normal vector  $V$  to  $\mathcal{S}_r$  at a smooth point, we let  $V_*$  denote the left translate of  $V$  to the origin. Let  $N_r$  denote the set of all such vectors  $V_r$ . Given the nature of the loop level sets, we have the following corollary of Theorem 2.5. For any  $\epsilon > 0$  there is some  $R$  such that  $N_r$  is contained in the  $\epsilon$ -tubular neighborhood of  $\Pi_X \cup \Pi_Y$  provided that  $r > R$ . We call this the *Lunar Principle* because  $\Pi_X \cup \Pi_Y$  intersects the unit sphere in a union of 4 spherical lunes. One does not really need the full force of Theorem 2.5 to deduce the Lunar Principle: A long geodesic tangent to a unit vector that is far from  $\Pi_X \cup \Pi_Y$  makes a corkscrew-like pattern and is quite far from distance minimizing.

## 2.7 Proof of the Projection Lemma

We call a map  $\eta$  between surfaces  $\theta$ -good if

$$\frac{\text{area}(\eta(S))}{\text{area}(S)} \geq \delta$$

for any measurable subset  $S$  in the domain. Mostly we are interested in the case when the domain is a smooth surface in Sol and the range is one of the coordinate planes in Sol. However, in the first result, we will consider planar surfaces in  $\mathbf{R}^3$ . The same projections  $\eta_X, \eta_Y, \eta_Z$  make sense as projections in  $\mathbf{R}^3$ .

**Lemma 2.6** *Let  $\Theta_X, \Theta_Y, \Theta_Z$  be positive numbers with  $\Theta_X^2 + \Theta_Y^2 + \Theta_Z^2 = 1$ . Let  $\Pi$  be any plane in  $\mathbf{R}^3$ . Then there is an  $I \in \{X, Y, Z\}$  such that the  $\eta_I$  is  $\Theta_I$ -good.*

**Proof:** It follows from the familiar fact that  $\|V \times W\|$  computes the area of the parallelogram spanned by two vectors  $V, W \subset \Pi$ , and from the Pythagorean Theorem, that there are 3 non-negative numbers  $r_X, r_Y, r_Z \geq 0$  so that  $r_X^2 + r_Y^2 + r_Z^2 = 1$ , and

$$A_\Pi(S) = r_X A_X(S) + r_Y A_Y(S) + r_Z A_Z(S). \quad (14)$$

Here  $S \subset \Pi$  is any measurable set and  $A_X(S)$  is the area of  $\Pi_X(S)$ , etc. If our claim is false then  $\Theta_I < r_I$  for all  $I \in \{X, Y, Z\}$ . But then

$$1 = \Theta_X^2 + \Theta_Y^2 + \Theta_Z^2 < r_X^2 + r_Y^2 + r_Z^2 = 1,$$

and we have a contradiction. ♠

Now we move the discussion to Sol.

**Lemma 2.7** *Let  $\Theta_X, \Theta_Y, \Theta_Z$  be positive numbers with  $\Theta_X^2 + \Theta_Y^2 + \Theta_Z^2 = 1$ . Let  $\Sigma$  be a smooth surface in Sol. Let  $p \in \Sigma$  be any point. Then for any  $\epsilon > 0$  there is a sufficiently small neighborhood  $U$  about  $p$  and some index  $I \in \{X, Y, Z\}$  such that  $\eta_I$  is  $\Theta_I$ -good on  $U$ .*

**Proof:** Given that Sol is homogeneous, and that the projections between parallel planes within the same coordinate foliation are area preserving, it

suffices to prove our result when  $p$  is the origin in Sol. But, in this case, the metric on Sol agrees with the Euclidean metric up to any given  $\epsilon$  we like. So, this special case follows from Lemma 2.6 and the differentiability of  $\Sigma$ . ♠

Now let us apply the Lunar Principle to the sphere  $\mathcal{S}_r$ . Given a smooth point  $p \in \mathcal{S}_r$ , the corresponding vector  $N_{p,0}$  lies quite near  $\Pi_X \cup \Pi_Y$ . The reason is that  $N_{p,0}$  either lies in  $\Pi_X \cup \Pi_Y$  or else in a loop level set of period greater than  $r$ , and such loop level sets lie near  $\Pi_X \cup \Pi_Y$ . Therefore, given any  $\epsilon > 0$  we can take  $r$  large enough so that there is a partition of the smooth points of  $\mathcal{S}_r$  into 3 measurable (or indeed piecewise smooth) regions

$$\mathcal{S}_r(I), \quad I \in \{X, Y, Z\}$$

with the following properties:

- The projection  $\eta_X : \mathcal{S}_r(X) \rightarrow \Pi_X$  is  $(\theta - \epsilon)$  good.
- The projection  $\eta_Y : \mathcal{S}_r(Y) \rightarrow \Pi_Y$  is  $(\theta - \epsilon)$  good.
- The projection  $\eta_Z : \mathcal{S}_r(Z) \rightarrow \Pi_Z$  is  $(\sqrt{1 - \theta^2} - \epsilon)$ -good.

Since the non-smooth subset of  $\mathcal{S}_r$  has area 0, the formula in the Projection Lemma follows immediately.

## 2.8 A Weaker Bound on Volume

This section is independent from the rest of the paper. Here we present, with minor modifications, Eryk Kopczyński's derivation of a weaker volume growth bound that is still sufficient to establish that Sol has volume entropy 1. I did not try for optimal constants.

**Lemma 2.8** *Suppose  $\gamma$  is a geodesic in Sol having length  $r$ . Let  $r_1$  be the length of  $\gamma$  that lies above the plane  $Z = 0$  and let  $r_2$  be the length of  $\gamma$  that lies below or in the plane  $Z = 0$ . Then the endpoint  $(x, y, z)$  of  $\gamma$  satisfies the bound  $|x| \leq e^{r_1} + r_2$  and  $|y| < e^{r_2} + r_1$ .*

**Proof:** We first consider two special cases. If  $\gamma$  stays above the plane  $\Pi_Z$  then the endpoint  $(x, y, z)$  satisfies the bounds  $|x| \leq e^r$  and  $|y| \leq r$ . Likewise, if  $\gamma$  stays below the plane  $\Pi_Z$  then the endpoint  $(x, y, z)$  satisfies the bounds  $|y| \leq e^r$  and  $|x| \leq r$ . In general, one can break  $\gamma$  into intervals

$\gamma_1, \dots, \gamma_k$ , for some  $k$ , such that each  $\gamma_j$  satisfies one of the two special cases just considered. Adding up the bounds from the special cases, we get the result advertised in the lemma. ♠

Set  $u = e^r$ . Note that  $r < u$ . Every point  $(x, y, z)$  in the ball of radius  $r$  satisfies

$$|x|, |y| \leq u + r, \quad |z| \leq r, \quad (|x| - r)(|y| - r) \leq u.$$

Let  $\Omega_r$  be the set of points satisfying these inequalities. For convenience we take  $r \geq 1$ . The volume of the part of  $\Omega_r$  where  $|x| \leq r + 1$  is bounded by

$$8r \times (r + 1) \times (u + r) < 32r^2u.$$

Likewise, the volume of the part of  $\Omega_r$  where  $|y| \leq r + 1$  is bounded by  $32r^2u$ . The volume of the part of the  $\Omega_r$  where  $|x| > r + 1$  and  $|y| > r + 1$  is

$$8r \int_1^u \frac{u}{x} dx \leq 8ru \log(u) = 8r^2u.$$

Therefore  $\Omega_r$  has volume at most  $72r^2e^r$ . But the ball of radius  $r$  is contained in  $\Omega_r$ .

### 3 The Hyperbolic Projections

#### 3.1 A Picture

Recall that  $\eta_X : \text{Sol} \rightarrow \Pi_X$  is the orthogonal projection onto the plane  $X = 0$ . Figure 3.1 shows the projection of (part of) the positive sector of the sphere  $\mathcal{S}_5$  into the plane  $\Pi_X$ . The smooth part of this sphere has a foliation by the images of the loop level sets under the Riemannian exponential map  $E$ . The grey curves are the projections of this foliation into  $\Pi_X$ . The black line segment is the projection of the set of singular points.

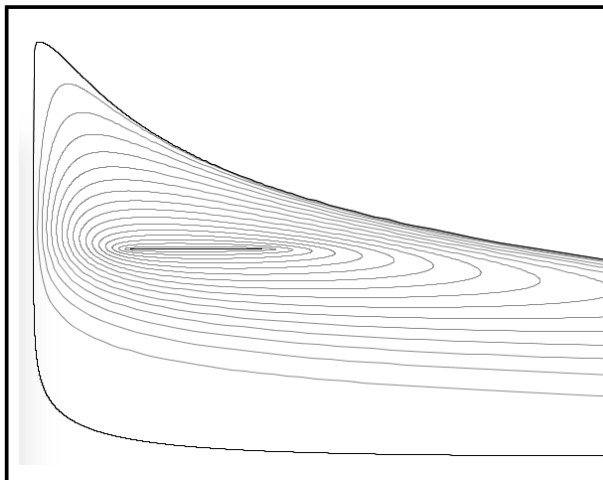


**Figure 3.1:** Projection into the plane  $\Pi_X$ .

It appears from the picture that the restriction of  $\eta_X$  to this sector is a homeomorphism onto its image. We will prove this result below. For convenience we take  $r > \pi\sqrt{2}$ .

#### 3.2 Area Bound

In this section we prove Projection Estimate 1. By symmetry, it suffices to prove the result for the projection  $\eta_X$  into the plane  $\Pi_X$ . Let  $\mathcal{S}_r^+$  denote the subset of  $\mathcal{S}_r$  consisting of points  $(x, y, z)$  with  $x \geq 0$ . Let  $\mathcal{H}_r$  denote the hyperbolic disk of radius  $r$  contained in the plane  $\Pi_X$  and centered at the origin. All the points in the interior of  $\mathcal{S}_r^+$  lie in the open positive sector. Because  $\Pi_X$  is a totally geodesic plane in  $\text{Sol}$ , we have  $\partial\mathcal{S}_r^+ = \partial\mathcal{H}_r$ . The following result immediately implies that  $A_{X,t} < \pi e^r$ .

**Lemma 3.1**  $\eta_X$  maps the interior of  $\mathcal{S}_r^+$  into the interior of  $\mathcal{H}_r$ .

**Proof:** If this is false, then there is a geodesic segment  $\gamma$  of length  $r$ , connecting  $(0, 0, 0)$  to some point  $p \in \mathcal{S}_r^+$  which remains entirely in the positive sector except for its initial point,  $(0, 0, 0)$ . The projection map  $\eta_X$  is distance non-increasing, and locally distance decreasing on any curve whose tangent vector is not in a plane of the form  $X = \text{const.}$ . This means that  $\eta_X(\gamma)$  is shorter than  $\gamma$ . But then  $\eta_X(\gamma)$  cannot reach the point  $\eta_X(p) \in \partial\mathcal{H}_r$ . ♠

### 3.3 Multiplicity Bound

In this section we prove Projection Estimate 2. As above, it suffices to prove this result for the projection  $\eta_X$  into the plane  $\Pi_X$ . To prove that  $N_{X,r} = 2$  it suffices, by symmetry, to show that  $\eta_X$  is an injective map from  $\mathcal{S}_r^+$  to  $\Pi_X$ . The basic strategy is to show that  $\eta_X$  is locally injective. We also know that  $\eta_X$  is the identity on the boundary of  $\mathcal{S}_r^+$ , which already lies in the plane  $X = 0$ . (It is the boundary of the hyperbolic disk on  $\Pi_X$  of radius  $r$  centered at the origin.) Our injectivity result then follows from the Disk Lemma in §2.

For convenience we take  $r > \pi\sqrt{2}$  in the next result, so that we don't have to discuss several cases. (The sphere  $\mathcal{S}_r$  is smooth for  $r < \pi\sqrt{2}$  and has 4 singular arcs for  $r > \pi\sqrt{2}$ .) The set of smooth points of  $\mathcal{S}_r$  is a union of 4 open "punctured" disks. In each case, we are removing an analytic arc from an open topological disk and what remains is smooth. Figure 4.1 shows (a portion of) the  $\eta_X$ -projections of the smooth points of  $\mathcal{S}_r$ .

**Lemma 3.2** *The differential  $d\eta_X$  is injective at all the smooth points in the interior of  $\mathcal{S}_r^+$*

**Proof:** Let  $S_r$  denote the subset of the sphere of radius  $r$  centered at the origin in the Lie algebra. As in the previous chapter, let  $S'_r$  denote the subset of  $S_r$  consisting of vectors which are either small or perfect. Let  $p \in S'_r$  be some point. We think of  $p$  as a vector, so that  $E(p) \in \mathcal{S}_r^+$ . Let  $T_p$  be the tangent plane to  $S'_r$  at  $p$ . Let  $N_p$  be the unit normal to  $T_p$ . Since the perfect geodesic segments are minimizers, the small geodesic segments are unique minimizers without conjugate points. So, at the corresponding points of  $S'_r$ , the differential  $dE_p$  is an isomorphism. We just have to show

that  $(1, 0, 0) \notin dE_p(T_p)$ . We will suppose that  $(1, 0, 0) \in dE_p(T_p)$  and derive a contradiction.

If  $(1, 0, 0) \in dE_p(T_p)$ , then the first component of  $dE_p(N_p)$  is 0, because  $dE_p(N_p)$  and  $dE_p(T_p)$  are perpendicular. Let  $\gamma_p$  be the geodesic segment corresponding to  $p$ . The vector  $dE_p(N_p)$  is the unit vector tangent to  $\gamma_p$  at its far endpoint – i.e., the endpoint not at the origin. This vector lies in the same left invariant vector field as the endpoint  $U_p$  of the flowline corresponding to  $p$ . If the first coordinate of  $U_p$  is 0, then the entire flowline lies in the plane  $X = 0$ . But then  $E(p) \in \partial\mathcal{S}_r^+$ . This is a contradiction. ♠

**Lemma 3.3** *The map  $\eta_X$  is locally injective at each singular point of  $\mathcal{S}_r^+$ .*

**Proof:** As we showed in [CS], the singular set in  $\mathcal{S}_r$  consists of 4 arcs of hyperbolas, each contained in the plane  $\Pi_Z$ . Each of these arcs lies in the interior of a different sector and is an arc of a hyperbola. These hyperbolas are all graphs of functions. The restriction of  $\eta_X$  to each hyperbola is therefore injective. We still need to see, however, that  $\eta_X$  is injective in neighborhoods of these singular sets, and not just on the singular sets. There are two cases.

**Case 1:** Consider a point  $p$  in the interior of the singular set in  $\mathcal{S}_r^+$ . By symmetry it suffices to consider the case when  $p$  is in the positive sector. The point  $p$  lies in the plane  $\Pi_Z$  and has its first two coordinates positive. There are exactly 2 points  $p_+, p_- \in S'_r$  such that  $E(p_+) = E(p_-) = p$ . These points have the form  $p_+ = (x, y, z)$  and  $p_- = (x, y, -z)$ . We called such points *partners*. In [CS, Lemma 2.8] we showed that  $dE_{p_\pm}$  is non-singular. This crucially uses the fact that  $p_\pm$  is a perfect vector whose third coordinate is nonzero. The same argument as in the previous lemma now shows that the linear map  $\eta_X \circ dE_{p_\pm}$  is an isomorphism from the tangent plane  $T_{p_\pm}$  to  $\mathbf{R}^2$ . But then  $\eta_X \circ E$  is a diffeomorphism when restricted to an open neighborhood  $U_\pm$  of  $p_\pm$  in  $S'_r$ .

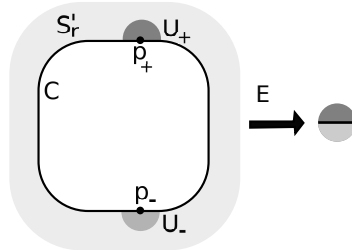


**Figure 3.2:** The neighborhoods  $U_+$  and  $U_-$ .

The sets  $U_{\pm}$  are disks with some of their boundary included. The portion of the included boundary consists of the perfect vectors in  $\partial S'_r$  near  $p_{\pm}$ . See Figure 3.2.

Let  $C$  be the component of  $\partial S'_r$  which contains  $p_+$  and  $p_-$ . The image  $E(U_+ - C)$  lies entirely below the plane  $\Pi_Z$  because the flowlines corresponding to vectors in  $U_+ - C$  nearly wind the entirely around their loop level set but omit a small arc near  $p_+$ . Likewise, the image  $E(U_- - C)$  lies entirely above the plane  $\Pi_Z$ . Hence  $\eta_X \circ E(U_+ - C)$  and  $\eta_x \circ E(U_- - C)$  are disjoint. Combining this what we know, we see that  $\eta_X$  is a homeomorphism in a neighborhood of  $p \in \mathcal{S}_r$ .

**Case 2:** Suppose that  $p$  is one of the endpoints of the singular set. This case is rather tricky to check directly. Suppose that there is some other point  $q \in \mathcal{S}_n$  such that  $\eta_X(p) = \eta_X(q)$ . By Lemma 3.1, the point  $\eta_X(p)$  is disjoint from the the hyperbolic circle  $\mathcal{S}_r^+ \cap \Pi_X$ . Hence  $q$  lies in the interior of  $\mathcal{S}_r^+$ . Since  $\eta_X$  is injective on the singular set,  $q$  must be a smooth point.

Since  $\eta_X(q) = \eta_X(p)$  and  $p \in \Pi_Z$ , we have  $q \in \Pi_Z$ . This means that  $q$  corresponds to some small symmetric flowline. The point  $q$  is contained in a maximal connected arc  $\mathcal{A} \subset \mathcal{S}_r^+$  consisting entirely of points corresponding to small symmetric flowlines. One endpoint of  $\mathcal{A}$  is  $p$ . The other endpoint lies in the plane  $X = 0$ . The point  $q$  lies somewhere in the interior of  $\mathcal{A}$ . The map  $\eta_X$  sends  $\mathcal{A}$  into the line  $X = Z = 0$  and from Lemma 3.3, the restriction of  $\eta_X$  to  $\mathcal{A}$  is locally injective. But a locally injective map from an arc into a line is injective. This contradicts the fact that  $\eta_X(p) = \eta_X(q)$ . ♠

Let  $D$  denote the quotient  $\mathcal{S}_r^+ / \sim$  where the equivalence relation  $\sim$  glues together partner points on the set of perfect vectors in  $\mathcal{S}_r^+$ . The space  $D$  is a topological disk, and  $h = \eta_X \circ E$  gives a map from  $D$  to  $\Pi_X$ . Combining Lemmas 3.2 and 3.3 we see that  $h$  is locally injective at each interior point of  $D$ . Moreover,  $h(\partial D)$  is an embedded loop, just the boundary of a hyperbolic disk in  $\Pi_X$ . By the Disk Lemma,  $h : D \rightarrow \Pi_X$  is injective. But  $E$  is a bijection from  $D$  to  $\mathcal{S}_r^+$ . Hence  $\eta_X : \mathcal{S}_r^+ \rightarrow \Pi_X$  is injective, as desired.

This completes the proof that  $N_{X,r} = 2$ .

## 4 Details about the Cut Locus Theorem

### 4.1 Concatenation

In the next several sections, we outline the proof of Theorem 2.5. Our exposition here is an abbreviated version of what appears in [CS].

Given a (finite) flowline  $g$  we write  $g = a|b$  if  $g$  is the concatenation of flowlines  $a$  and  $b$ . That is,  $a$  is the initial part of  $g$  and  $b$  is the final part. We call  $g$  *symmetric* if the endpoints of  $g$  have the form  $(x, y, z)$  and  $(x, y, -z)$ .

Let  $\Lambda_g$  denote the endpoint of the geodesic segment associated to  $g$ , when this geodesic segment starts at the origin. It follows from left-invariance of the metric that

$$\Lambda_g = \Lambda_a * \Lambda_b. \quad (15)$$

Since the third coordinates of elements of Sol commute, we have

$$\pi_Z(\Lambda_g) = \pi_Z(\Lambda_a) + \pi_Z(\Lambda_b). \quad (16)$$

Here  $\pi_Z(x, y, z) = z$ . More formally,  $\pi_Z$  is the quotient map from Sol to the quotient  $\text{Sol}/\Pi_Z$ . Here  $\Pi_Z$  is not just a Euclidean plane in Sol but also a maximal normal subgroup. The integral form of Equation 16 is

$$\pi_Z(\Lambda_g) = \int_0^T z(t) dt. \quad (17)$$

Here we have set  $g = (x, y, z)$ , and  $T$  is the total time that  $g$  takes to get from start to finish.

These equations have a variety of consequences, which we work out in detail in [CS, §2].

1. If  $g$  is a small flowline then  $g$  is symmetric if and only if  $\pi_Z(\Lambda_g) = 0$ . Moreover, the geodesic segment corresponding to a small symmetric flowline only intersects  $\Pi_Z$  at its endpoints.
2. If  $g$  is a perfect flowline then  $\pi_Z(\Lambda_g) = 0$ . This follows from the fact that  $g = a|b$  where  $a$  and  $b$  are both small symmetric.
3. If  $V_{\pm} = (x, y, \pm z)$ , then  $V_+$  is perfect if and only if  $V_-$  is perfect. Furthermore  $E(V_+) = E(V_-)$ . This is because the corresponding flowlines  $g_+$  and  $g_-$  can be written as  $g_+ = a|b$  and  $g_- = b|a$  where  $a$  and  $b$  are both small symmetric. But then  $\Lambda_a$  and  $\Lambda_b$  are horizontal translations

in Sol and hence commute. Hence  $\Lambda_{g_+} = \Lambda_{g_-}$ . We call  $V_+$  and  $V_-$  *partners*.

4. Suppose  $V_1$  and  $V_2$  are perfect vectors such that  $V_1/\|V_1\|$  and  $V_2/\|V_2\|$  lie in the same loop level set. Let  $E(V_i) = (a_i, b_i, 0)$ . We call  $\sqrt{a_i b_i}$  the *holonomy* of  $V_i$ . Letting  $g_1$  and  $g_2$  be the corresponding flowlines, we can write  $g_1 = a|b$  and  $g_2 = b|a$  where  $a$  and  $b$  are both small. But then  $\Lambda_{g_1} = (a_1, b_1, 0)$  and  $\Lambda_{g_2} = (a_2, b_2, 0)$  are conjugate in Sol. This gives  $a_1 b_1 = a_2 b_2$ . Hence  $V_1$  and  $V_2$  have the same holonomy.
5. Given  $V = (x, y, z)$  we define  $\sigma(V) = y/x$ . We prove that if  $V$  is a perfect vector, then  $\sigma(E(V)) = 1/\sigma(V)$ . We call this the Reciprocity Lemma. The proof is a more subtle working out of the consequences of the conjugacy idea discussed in Item 4.

## 4.2 Outline of the Proof

With these preliminaries out of the way, we turn directly to the proof of Theorem 2.5. Item 3 in §4.1 shows that the perfect geodesic segments corresponding to vectors of the form  $(x, y, z)$  where  $z \neq 0$  are not unique distance minimizers. It also follows from Item 3 that perfect geodesic segments corresponding to vectors of the form  $(x, y, 0)$  have conjugate points. Hence, large geodesic segments cannot be distance minimizers. This essentially proves half of Theorem 2.5.

The second half of Theorem 2.5, the converse, says that a small or perfect geodesic segment is a distance minimizer. Since every small geodesic segment is contained in a perfect geodesic segment, it suffices to prove that perfect geodesic segments are distance minimizers.

We first prove [CS, Corollary 2.10]: The map  $E$  is injective on the set of perfect vectors with positive coordinates. This step has 2 ideas. We first show (following [G]) that the holonomy is a monotone function of the loop level set. So, if  $E(V_1) = E(V_2)$  then  $V_1/\|V_1\|$  and  $V_2/\|V_2\|$  lie in the same loop level set. We also have  $\sigma(V_1) = \sigma(V_2)$ , by Item 5 above. This forces  $V_1 = V_2$ .

We finish the proof by showing that if  $V$  is perfect and  $W$  is small then it is impossible for  $E(V) = E(W)$ . This is really the heart of [CS]. The argument involves the system of nonlinear ODEs we introduce in §4.3. It will turn out that the argument in this paper involves a deeper study of these same ODEs.

Let us go back to the argument. By symmetry, we can restrict ourselves to the case when  $V$  and  $W$  both lie in the positive sector. Let  $M$  and  $\partial M$  respectively denote the set of small and perfect vectors. We show that  $E(\partial M)$  is contained in a subset  $\partial N \subset \Pi_Z$ . The boundary of  $\partial N$ , which we denote by  $\partial_0 N$ , is the graph of a smooth function in polar coordinates. The yellow region in Figure 3.1 shows part of the portion of  $\partial N$  that lies in the positive sector. See Figure 5.1 for an expanded view. There 3 symmetrically placed components in the other sectors which we are not showing.

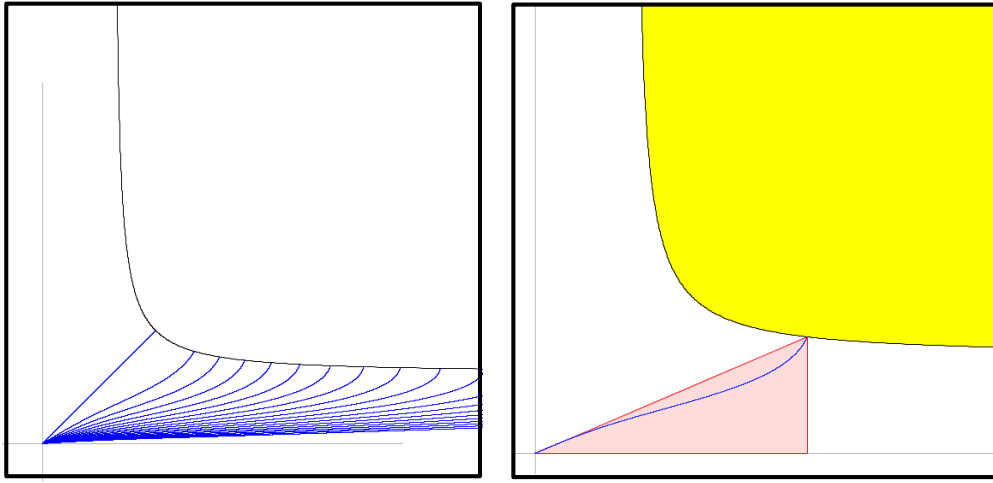


**Figure 3.1:**  $\partial_0 N_+$  (black),  $\partial N_+$  (yellow),  $\Lambda_L$  (blue), and  $\Delta_L$  (red).

If we suppose that  $W$  is small and  $E(W) = E(V)$  then the flowline corresponding to  $W$  must be small symmetric. We can arrange all the small symmetric flowlines in a given loop level set into two curves. One of the curves corresponds to small symmetric flowlines whose initial endpoint has positive  $Z$ -coordinate. Given the loop level set of period  $L$  in the positive sector, we let  $\Lambda_L$  denote the image, under  $E$ , of the corresponding vectors. The blue curves in Figure 3.1 show  $\Lambda_L$  for various choices of  $L$ .

On the right side of Figure 3.1 we focus on  $\Lambda_5$ . We also draw the right triangle  $\Delta_5$  whose endpoints are the endpoints of  $\Lambda_5$ . We define the triangle  $\Delta_L$  for other values of  $L$  in the same way. In [CS, §3] we prove that  $\Lambda_L \subset \Delta_L$  and that the interior of  $\Lambda_L$  lies in the interior of  $\Delta_L$ . Finally, we show that  $\partial_0 N$  intersects  $\Delta_L$  only at the top vertex. These ingredients combine to show that  $\Lambda_L \cap \partial N = \emptyset$ , and this shows that  $E(V)$  and  $E(W)$  cannot be equal.

### 4.3 The Differential Equation

We will now go into more detail about how the Bounding Triangle Theorem is proved. Let  $\ell = L/2$ . We consider the *backwards flow* along the structure field  $\Sigma$ , namely

$$x' = -xz, \quad y' = +yz, \quad z' = x^2 - y^2, \quad (18)$$

with initial conditions  $x(0) > y(0) > 0$  and  $z(0) = 0$  chosen so that the point is in the loop level set of period  $L$ . (We will often denote these functions as  $x_L$ , etc.) We let  $g_t$  be the small symmetric flowline whose endpoints are  $(x(t), y(t), z(t))$  and  $(x(t), y(t), -z(t))$ . Then

$$\Lambda_L(t) = (a(t), b(t), 0) = \Lambda_{g_t}.$$

Taking the derivative, we have

$$(a', b', 0) = \Lambda'_L(t) = \lim_{\epsilon \rightarrow 0} \frac{\Lambda_L(t + \epsilon) - \Lambda(t)}{\epsilon},$$

$$\Lambda_L(t + \epsilon) \approx (\epsilon x, \epsilon y, \epsilon z) * (a, b, 0) * (\epsilon x, \epsilon y, -\epsilon z).$$

The approximation is true up to order  $\epsilon^2$  and  $(*)$  denotes multiplication in Sol. A direct calculation gives

$$a' = 2x + az, \quad b' = 2y - bz. \quad (19)$$

The initial conditions are  $a(0) = b(0) = 0$ . (We will often denote these functions as  $a_L$  and  $b_L$ .)

**Lemma 4.1** *For any  $r \geq 0$  we have*

$$a(r)x(r) = \int_0^r 2x^2 dt, \quad b(r)y(r) = \int_0^r 2y^2 dt.$$

**Proof:** We have  $(ax)' = 2x^2$  and  $(by)' = 2y^2$ . Also  $a(0) = b(0) = 0$ . Now we simply integrate. ♠

**Lemma 4.2**

$$\frac{b(0)}{a(0)} = \frac{b(\ell)}{a(\ell)}. \quad (20)$$

**Proof:** This comes from L’hopital’s rule and the Reciprocity Lemma. Let us take the opportunity to give a swift proof here. (This is another proof of the Reciprocity Lemma in a special case.) By two applications of Lemma 4.1, we have

$$a(\ell)x(\ell) = \int_0^\ell 2x^2 dt, \quad b(\ell)y(\ell) = \int_0^\ell 2y^2 dt.$$

But these two integrals are equal, by symmetry. Hence  $a(\ell)x(\ell) = b(\ell)y(\ell)$ . Finally, we have  $x(0) = y(\ell)$  and  $y(0) = x(\ell)$  by symmetry. Combining these equations gives the result. ♠

The function  $b(t)/a(t)$  has the same value at  $t = 0$  and  $t = \ell$ . To finish the proof, we just have to show that  $b(t)/a(t)$  cannot have a local maximum. This boils down to the fact that  $ab'' - ba'' = 2ab(y^2 - x^2)$ , a quantity which is negative for  $t < \ell/2$  and positive for  $t > \ell/2$ . These properties, together with the fact that  $a' > 0$ , force  $\Lambda_L \subset \Delta_L$ . See [CS, §3] for more details.

## 5 More Information about the ODE

In this chapter we further explore the ODE we introduced in the previous chapter. The results here do not appear in [CS]. However, they are rather similar in spirit to some of the results there. Lemma 4.1 above has a lot of juice in it, and we want to squeeze some more out. The estimates here will be useful when we consider the projections of the Sol spheres into the Euclidean plane  $\Pi_Z$ .

### 5.1 Bounding the Coordinates

In the next lemma,  $2^*$  refers to a number which we can make as close as we like to 2 by taking  $L$  sufficiently large. This result says that the boundary of the yellow region in Figure 3.1 asymptotes to the lines  $X = 2$  and  $Y = 2$ .

**Lemma 5.1**  $b(\ell) < 2^*$ .

**Proof:** From Lemma 4.1 and symmetry we have

$$y(\ell)b(\ell) = \int_0^\ell y^2 = \int_0^{\ell/2} (x^2 + y^2)dt.$$

The last equality follows from the fact that the function  $t \rightarrow x^2(t) + y^2(t)$  is periodic with period  $\ell/2$ . Since  $b(\ell) \sim 1$  for large  $L$ , it suffices to prove that the integral on the right approaches 1 as  $L \rightarrow \infty$ .

We have

$$\int_0^{\ell/2} (x^2 + y^2)dt = \int_0^{\ell/2} (x^2 - y^2)dt + 2 \int_0^{\ell/2} y^2 dt. \quad (21)$$

Now observe that

$$\int_0^{\ell/2} (x^2 - y^2)dt = \int_0^{\ell/2} z' dt = z(\ell/2) - z(0) = z(\ell/2) \sim 1. \quad (22)$$

To finish the proof, it suffices to show that

$$\int_0^{\ell/2} y^2 dt \sim 0. \quad (23)$$

Let  $\alpha$  be such that  $(x(0), y(0), 0)$  lies in the same loop level set as

$$(\alpha, \alpha, \sqrt{1 - 2\alpha^2}).$$

Then  $y \leq \alpha$  on  $[0, \ell/2]$  because  $y$  is monotone increasing on this interval. Hence, by Equation 11 and some algebraic manipulation,

$$\int_0^{\ell/2} y^2 dt \leq L_\alpha \times \alpha^2 = 2\alpha \sqrt{\frac{4\alpha^2}{1 + 2\alpha^2}} \times \mathcal{K}\left(\frac{1 - 2\alpha^2}{1 + 2\alpha^2}\right).$$

Setting  $m = \frac{1 - 2\alpha^2}{1 + 2\alpha^2}$ , we see that

$$\int_0^{\ell/2} y^2 dt \leq 2\alpha \sqrt{1 - m} \times \mathcal{K}(m). \quad (24)$$

As  $L \rightarrow \infty$  we have  $\alpha \rightarrow 0$  and  $m \rightarrow 1$  and  $\mathcal{K}(m) \sim -\log(1 - m)/2$ . Hence, the right hand side of Equation 24 tends to 0 as  $L \rightarrow \infty$ . ♠

**Remark:** We also have  $a(\ell)b(\ell) \sim e^\ell$ , as discussed in [CS, §3.7] and also on [G, p 75].

**Lemma 5.2**  $a(L) = 2b(\ell)$ .

**Proof:** We have

$$a(L)x(L) = \int_0^L 2x^2 dt = \int_0^\ell 2x^2 dt + \int_\ell^L 2x^2 dt = 2 \int_0^\ell 2y^2 dt = 2b(\ell)y(\ell).$$

Hence

$$a(L)x(L) = 2b(\ell)y(\ell).$$

But  $x(L) = y(\ell)$ , so we can cancel these terms to get the desired equality. ♠

## 5.2 The Doubling Lemma

It will be useful for us to consider flowlines which end on the plane  $Z = 0$ . These are the initial halves of symmetric flowlines. Here *doubling* refers to comparing the first half of a symmetric flowline with the whole thing.

Let  $\underline{g}_t$  denote the first half of the flowline  $g_t$ ; it connects the initial point of  $g_t$  to the midpoint of  $g_t$ . Say that the coordinates of  $\Lambda_{\underline{g}_t}$  are  $(\underline{a}(t), \underline{b}(t), \underline{c}(t))$ . The coordinate  $\underline{c}(t)$  is typically nonzero, but we do not care about it. Define

$$\underline{\Lambda}_L(t) = (\underline{a}_L(t), \underline{b}_L(t)) \subset \mathbf{R}^2. \quad (25)$$

In the next lemma we identify  $\Pi_Z$  with  $\mathbf{R}^2$ .

**Lemma 5.3 (Doubling)**  $\underline{\Lambda}(t) = \frac{1}{2}\underline{\Lambda}_L(t)$ .

**Proof:** We have

$$(\underline{a}', \underline{b}', \underline{c}') = \lim_{\epsilon \rightarrow 0} \frac{\underline{\Lambda}_L(t + \epsilon) - \underline{\Lambda}(t)}{\epsilon}, \quad \underline{\Lambda}_L(t + \epsilon) \approx (\epsilon x, \epsilon y, \epsilon z) * (a, b, c).$$

Taking the limit, we find that

$$\underline{a}' = z + \underline{a}x, \quad \underline{b}' = z - \underline{b}x. \quad (26)$$

(Also  $\underline{c}' = z$ . We have the same initial conditions  $\underline{a}(0) = \underline{b}(0)$  as above. Now notice that this solution to this equation is given by  $\underline{a} = a/2$  and  $\underline{b} = b/2$ . ♠

**Corollary 5.4**  $b(\ell) = \underline{a}(L)$ .

**Proof:** We combine the Doubling Lemma and Lemma 5.2 to get the equation  $b(\ell) = a(L)/2 = \underline{a}(L)$ . ♠

Now we give some applications, which show how the Doubling Lemma and our asymptotics above give us some specific information about some geodesic segments in Sol. Let  $f(r, L)$  denote the flowline of length  $r$  on the loop level set of period  $L$  which ends at the point  $(x, y, 0)$  with  $x > y$ . Let

$$\Upsilon_r(L) = \Lambda_{f(r, L)}.$$

This is the endpoint of the corresponding geodesic segment. The *isochronal curve*  $L \rightarrow \Upsilon_r(L)$ , for  $L \in [r, \infty)$  will be a central object later in the paper.

1. We have  $\Upsilon_r(r) \sim (2, e^{r/2}/2, 0)$  by Lemma 5.1 and the remark after Lemma 5.1 and symmetry.

2. We have  $\Upsilon_r(2r) \sim (e^r/4, 1, *)$  by Case 1, and symmetry, and the Doubling Lemma.
3. We have  $\Upsilon_r(4r) \sim (e^r/2, *, *)$ .

We do not need Item 3 for any purpose, so we will be a bit sketchy with the proof. The small symmetric flowline of which  $f(r, 4r)$  is the first half starts at  $(0, 0, z)$  and ends at  $(0, 0, -z)$  for the appropriate choice of  $z$ . The corresponding geodesic segment  $\gamma$  of length  $2r$  connects the origin to a point in  $\Pi_Z$  and remains nearly tangent to  $\Pi_Y$ . Also,  $\gamma$  starts and ends nearly vertically. In fact,  $\gamma$  is asymptotic to the geodesic segment considered in Lemma 2.1. Thus, the first coordinate of the far endpoint of  $\gamma$  is asymptotic to  $e^r$ . By the Doubling Lemma, the first coordinate of  $\Upsilon_r(4r)$  is asymptotic to  $e^r/2$ .

For what it is worth, the second coordinate tends to 0 as  $r \rightarrow \infty$ . To see this, note that the product of the first two coordinates of  $\gamma$  is, by Lemma 4.1,

$$\frac{4}{x(r)y(r)} \int_0^r x^2 dt \int_0^r y^2 dt \sim \frac{4}{x(r)y(r)} \int_0^r y^2 dt < \frac{4ry(r)^2}{x(r)y(r)} = 4r.$$

The asymptotic estimate  $\sim$  is Equations 22 – 23. The last inequality comes from the monotone increasing nature of  $y(t)$  for  $t \in [0, r]$ . The equality comes from the fact that  $x(r) = y(r)$ .

## 6 The Euclidean Projection

### 6.1 Notation

We introduce some notation that we use through out the chapter. We will consider some quantity  $F$  that depends on the variable  $r$  or the variable  $L$ . The statement  $F < \zeta^*$  means that, for any  $\zeta^* > \zeta$  we can make  $F < \zeta^*$  provided that we take  $r$  or  $L$  sufficiently large.

### 6.2 The Cut Locus Image

Figure 6.1 shows a more of the yellow region in Figure 3.1. In this section we will prove a result which is equivalent to the statement that the horizontal asymptote of the boundary curve is the line  $y = 2$ . Similarly, the vertical asymptote is the line  $x = 2$ .

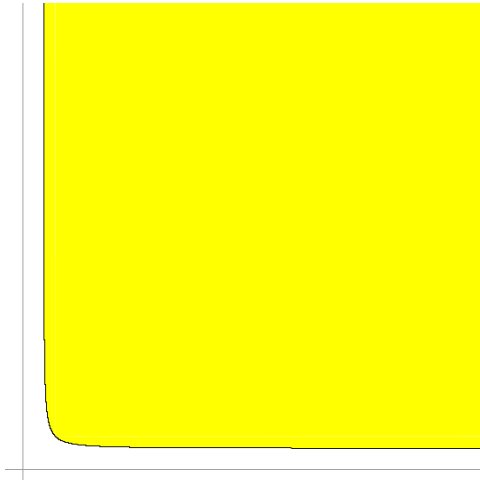


**Figure 6.1:**  $\partial N$  in the positive quadrant.

Say that a vector is *positive* if all its coordinates are positive. Say that a vector is *distinguished* if its corresponding flowline is contained in a small symmetric flowline with the same initial point. That is, the flowline corresponding to the distinguished vector can be prolonged until it is a small symmetric flowline. In particular, distinguished vectors are small.

**Theorem 6.1 (Asymptotic)** *If  $V$  is a distinguished positive vector whose corresponding flowline is contained in a loop level set of period  $L$ , then  $E(V) = (a, b, 0)$  has the property that  $b \in (0, 2^*)$ .*

**Proof:** First consider the special case when  $V$  corresponds to a small symmetric flowline. Then  $b = b_L(t)$  for some  $t \leq \ell$ . By the Bounding Triangle Theorem and Lemma 5.1,  $b_L(t) \leq b_L(\ell) < 2^*$ .

Now consider the case when  $V$  is an arbitrary distinguished positive vector. There is some  $\lambda \geq 1$  so that  $\lambda V$  corresponds to a small symmetric flowline. The  $X$  and  $Y$  coordinates of the curve  $t \rightarrow E(tV)$  are increasing functions because it is impossible for the geodesic associated to  $V$  to be tangent to the hyperbolic foliations of Sol. (Otherwise this geodesic would be trapped inside a leaf of the foliation for all time.) In particular, the second coordinate of  $E(V)$  is less or equal to the second coordinate of  $E(\lambda V)$ , which is in turn less than  $2^*$  by the special case. ♠

### 6.3 The Area Bound

Our main goal is to show that  $A_Z(\mathcal{S}_r) < 16^*e^r$ . Lemma 6.2 below is the main ingredient in the proof. This result says that when  $(a, b) \in \eta_Z(\mathcal{S}_r)$  we have  $\min(a^2b, ab^2) < 2^*e^r$ . Figure 6.2 indicates the plausibility of this estimate. Figure 6.2 shows the projection of (part of the positive sector of)  $\mathcal{S}_5$  into the plane  $\Pi_Z$ . The small black arc of a hyperbola is the projection of the singular set. The outer black curve is  $\min(xy^2, x^2y) = e^5$ .

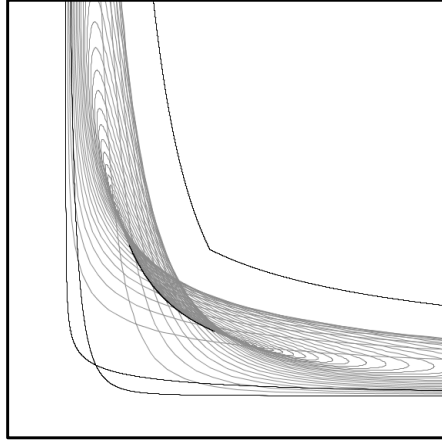


**Figure 6.2:** Projection into the plane  $\eta_Z$ .

**Lemma 6.2** *Let  $(a, b, c) = E(V)$ , where  $V$  is a small or perfect vector of length  $r$ . Then  $\min(ab^2, a^2b) < 2^*e^r$  and  $\max(a, b) < (1/2)^*e^r$ .*

**Proof:** Note that as  $r \rightarrow \infty$ , the period of the loop level set containing  $V$  also tends to  $\infty$ . This makes the Asymptotic Lemma available to us.

Let  $\gamma$  be the geodesic segment corresponding to  $V$ . Let  $g$  be the flowline corresponding to  $V$ . We can write  $g = g_1|g_2$  where one of two things is true:

- $g_1$  is distinguished and  $g_2$  is empty.
- $g_1$  is small symmetric and  $g_2$  is distinguished.

After interchanging the roles of  $X$  and  $Y$  if necessary, we reduce to 2 cases.

**Case 1:** Let  $\gamma_1$  be the geodesic segment corresponding to  $g_1$ , having endpoint  $(a, b, c)$ . By the hyperbolic estimates, we know that  $\eta_Y(\gamma_1)$  lies in the hyperbolic disk  $D_r$  in  $\Pi_Y$  centered at the origin. By Lemma 2.2, we have  $a < (1/2)^*e^r$ . We also have  $b < 2^*$  by the Asymptotic Theorem. Hence  $ab^2 < 2^*e^r$ . We also see that  $\max(a, b) < (1/2)^*e^r$ .

**Case 2:** Let  $\gamma_1$  and  $\gamma_2$  respectively be the geodesic segments corresponding to  $g_1$  and  $g_2$ . Let  $r_j$  be the length of  $\gamma_j$ . Let  $(a_j, b_j)$  be the projection to  $\eta_Z$  of the far endpoint of  $\gamma_j$ .

Let  $\gamma'_1$  be the geodesic segment which is the first half of  $\gamma_1$ , in terms of length. So,  $\gamma'_1$  and  $\gamma_1$  have the same initial endpoint (the origin) but  $\gamma'_1$  has length  $r_1/2$ . Let  $(a'_1, b'_1)$  be the far endpoint of  $\eta_Z(\gamma'_1)$ . Once  $r$  is large enough we have the following:

- By Lemma 2.1,  $a_1 \leq e^{r_1/2} - e^{-r_1/2}$ .
- By the Asymptotic Theorem,  $b_1 < 2^*$ .
- By Lemma 2.2 and symmetry,  $b_2 \leq (e^{r_2} - e^{-r_2})/2$ .
- By symmetry and the Asymptotic Theorem,  $a_2 < 2^*$ .

Combining these observations, we have

$$a \leq 2^* + e^{r_1/2} - e^{-r_1/2}, \quad b \leq 2^* + (e^{r_2} - e^{-r_2})/2. \quad (27)$$

We have  $r_1 + r_2 = r$ . We get right away that  $\max(a, b) < (1/2)^*e^r$ .

Now we consider  $a^2b$ . Suppose first that both  $r_1$  and  $r_2$  tend to  $\infty$ . In this case  $a < 1^*e^{r_1/2}$  and  $b < (1/2)^*e^{r_2}$ . But then  $a^2b < (1/2)^*e^r$ .

When  $r_1$  is bounded and  $r_2 \rightarrow \infty$ ,

$$a^2 b < (1/2)^* a^2 e^{r_2} = e^r \times \left( \frac{1}{2} + \frac{e^{-2r_1}}{2} - 2e^{-3r_1/2} + e^{-r_1} + 2e^{-r_1/2} \right) < 2^* e^r.$$

The last inequality follows from a bit of calculus.

When  $r_2$  is bounded and  $r_1 \rightarrow \infty$  we have  $a < 1^* e^{(r-r_2)/2}$ . This gives

$$a^2 b < 1^* e^r \times \left( 1 - e^{-2r_2} + 2e^{2r_2} \right) < 2^* e^r.$$

This completes the proof. ♠

Once  $r$  is sufficiently large, the sphere  $S'_r$  consists entirely of small and perfect vectors either contained in the planes  $\Pi_X$  and  $\Pi_Y$  or else lying in loop level sets whose period is so large that Lemma 6.2 holds for them. Lemma 6.2 shows that the projection of the positive sector of  $\mathcal{S}_r$  lies in the region  $\Omega_r$  defined by the following inequalities.

$$X, Y \in [0, (1/2)^* e^r], \quad \min(xy^2, yx^2) = 2^* e^r. \quad (28)$$

We set  $x_0 = y_0 = (2^* e^r)^{1/3}$ . The region  $\Omega_r$  is the union of the square  $[0, x_0] \times [0, y_0]$ , whose area is  $0^* e^r$ , and two other regions which are swapped by reflection in the main diagonal  $x = y$ . One region lies underneath the graph  $y = (2^* e^r/x)^{1/2}$  starting at  $x = x_0$  and ending at  $x = (1/2)^* e^r$ . This region has area

$$\sqrt{2^*} e^{r/2} \int_{x_0}^{(1/2)^* e^r} \frac{dx}{\sqrt{x}} < \sqrt{2^*} e^{r/2} \times 2 \times \sqrt{(1/2)^* e^r} < 2^* e^r, \quad (29)$$

once  $r$  is large. Hence  $\Omega_r$  has area at most  $4^* e^r$ . Recalling that  $\Omega_r$  contains the projection of the positive sector of  $\mathcal{S}_r$ , which is  $1/4$  of the whole sphere, we see that  $A_X(\mathcal{S}_r) < 16^* e^r$ .

**Remark:** The set  $\eta_X(\mathcal{S}_r)$  contains the region  $G_r$  above the  $X$ -axis, underneath the arc  $\Upsilon_r[2r, 4r]$  discussed in §5.2, and to the right of the line  $x = e^2 \times e^{r/2}$ . Given our Embedding Theorem below, and the estimates in §5.2, we see that the upper boundary of  $G_r$  is the graph of a decreasing function whose domain has length  $e^r/4^*$  and whose minimum is asymptotic to 1. Thus  $G_r$  contains a rectangle of area  $e^4/4^*$ . Hence  $A_X(\mathcal{S}_r) > (2/1^*)e^r$ .

## 6.4 The Yin Yang Curve

Given  $r$ , we define the *yin-yang curve*  $Y_r$  to be the set of points in  $S'_r$  where the differential  $d(\eta_Z \circ E)$  is singular. For  $r \leq \pi\sqrt{2}$  the the curve  $Y_r$  is connected. For  $r > \pi\sqrt{2}$ , the curve has 2 disjoint components interchanged by the map  $(x, y, z) \rightarrow (y, x, -z)$ .

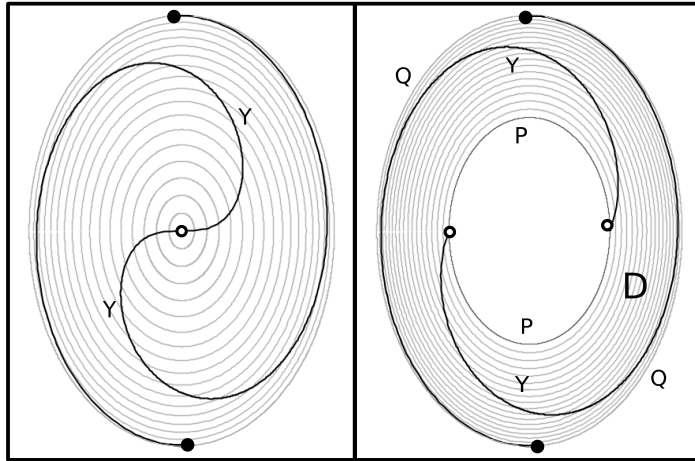


**Figure 6.3:** The yinyang curves for  $r = \pi\sqrt{2}$  and  $r = 5$ .

Figure 6.3 shows the yin-yang curves for  $r = \pi\sqrt{2}$  and for  $r = 5$ . In Figure 6.3, we are projecting the unit sphere in  $\mathbf{R}^3$  onto the plane through the origin perpendicular to the vector  $(1, -1, 0)$ . The loop level sets all project to ellipses having aspect ratio  $\sqrt{2}$ . On the right side of Figure 6.3, the ellipse labeled  $P$  is the set of perfect vectors on  $S'_5$ . The ellipse labeled  $Q$  is the intersection of the positive sector of the unit sphere with the planes  $X = 0$  and  $Y = 0$ . Notice that  $P_r \cup Y_r \cup Q_r$  divides  $S'_r$  into a union of 2 disks. The map  $\eta_Z \circ \Pi$  is nonsingular on the interior of these disks and hence a local diffeomorphism. This is what is important for our Projection Estimate 4.

Referring to Figure 6.3, the union  $Y_r \cup P_r \cup Q_r$  separates the positive sector of  $S'_r$  into 2 components. The map  $(x, y, z) \rightarrow (x, y, -z)$  interchanges these components. Let  $D_r$  be either of these disks. Below, we will describe more clearly which of the two choices we take to be  $D_r$ . Figure 6.4 shows  $\eta_Z \circ E(D_5)$ . Essentially this is “half” of Figure 6.2.

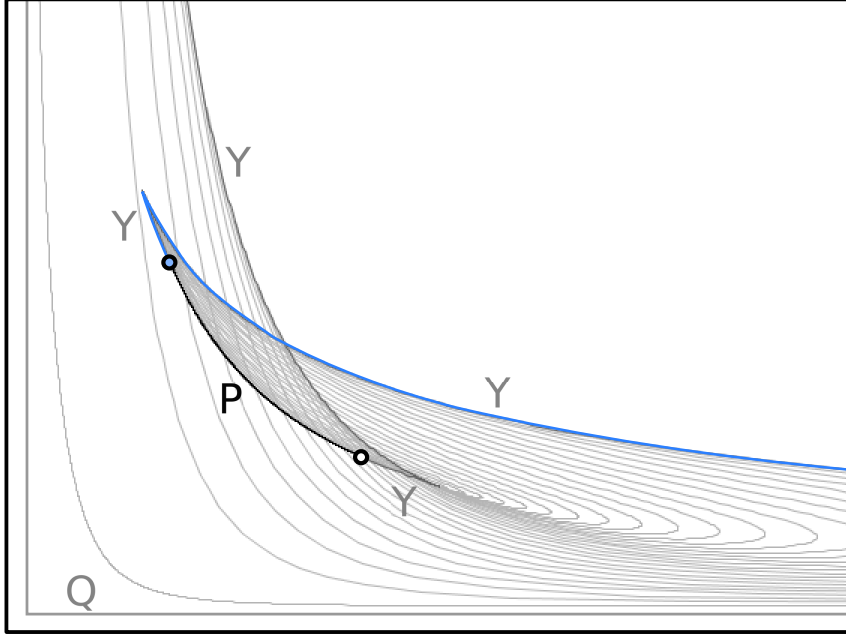


**Figure 6.4:** The image  $\eta_Z \circ E(D_5)$ .

The region labeled  $Y$  in Figure 6.3 is the image  $\eta_Z \circ E(Y_r)$ . We define  $\Upsilon_r = \eta_Z \circ E(Y_r^*)$ , where  $Y_r^*$  is the component of  $Y_r$  whose endpoint in  $\Pi_X$  is a point of the form  $(x_r, y_r, 0)$  with  $x_r > y_r$ . We have drawn  $\Upsilon_r$  in blue in Figure 6.4.

The map  $L \rightarrow \Upsilon_r(L)$  is a smooth, and indeed real analytic, map. We say that a *cuspl* of this map is a point where the map is not regular. So, away from the cusps,  $\Upsilon_r$  is a smooth regular curve. Figure 6.3 suggests that  $\Upsilon_5$  just has a single cusp. We prove the following result in the next chapter.

**Theorem 6.3 (Embedding)** *For  $r$  sufficiently large, the curve  $\Upsilon_r$  has a single cusp, and negative slope away from a single cusp. The cusp  $\kappa_r = (a_r, b_r, c_r)$  satisfies the bounds  $a_r < 2^*$  and  $b_r < (e^2/2)^* e^{r/2}$ .*

## 6.5 The Multiplicity Bound

The image  $\eta_Z \circ E(\partial D_r)$  is a piecewise analytic loop. We will show that this loop winds at most twice around any point in the plane that it does not contain. Referring to §2.3, we apply the Disk Lemma to  $h = \eta_Z \circ E$  and  $\Delta = D_r$ . This tells us that  $\eta_Z \circ E$  is at most 2-to-1 on  $D_r$ . But then  $\eta_Z \circ E$  is

at most 4-to-1 on the positive sector of  $S'_r$ . Hence  $\eta_Z$  is at most 4-to-1 on the positive sector of  $\mathcal{S}_r$ . Since the different sectors project into  $\eta_Z$  disjointly, we see that  $\eta_Z$  is at most 4-to-1 on all of  $\mathcal{S}_r$ . This establishes our estimate  $N_Z(\mathcal{S}_r) = 4$ .

Now we turn to the analysis of the image  $\eta_Z \circ E(\partial D_r)$ . Define

$$\Phi_r = E \circ \eta_Z(P_r). \quad (30)$$

Also, let  $R(x, y, z) = (y, x, -z)$ . The image  $\eta_Z \circ E(\partial D_r)$  is invariant under  $R$ . It is the union of 5 analytic arcs:

- An arc of the  $X$ -axis connecting the origin to the endpoint of  $\Upsilon_r$ .
- $\Upsilon_r$ .
- $\Phi_r$ .
- $R(\Upsilon_r)$ .
- An arc of the  $Y$ -axis connecting an endpoint of  $R(\Upsilon_r)$  to the origin.

Note that  $\Upsilon_r \cup \Phi_r \cup R(\Upsilon_r)$  is a piecewise analytic arc that has its endpoints in the coordinate axes and otherwise lies in the positive quadrant. The Embedding Theorem says that  $\Upsilon_r$  has negative slope, and is smooth and regular away from a single cusp. By symmetry, the Embedding Theorem also applies to  $R(\Upsilon_r)$ .

The cusps serve as natural vertices for our loop, so we make some new definitions which take the cusps into account. Let  $\Phi_r^*$  denote the portion of  $\Upsilon_r \cup \Phi_r \cup R(\Upsilon_r)$  that lies between the two cusps. Let  $\Upsilon_r^* = \Upsilon_r - \Phi_r^*$ . The loop  $\eta_Z \circ E(\partial D_r)$  has the same 5-part description as above, with  $\Upsilon_r^*$  and  $\Phi_r^*$  used in place of  $\Upsilon_r$  and  $\Phi_r$ .

We will prove below that  $\Upsilon_r^* \cup \Phi_r^*$  is embedded. By symmetry,  $\Phi_r^* \cup R(\Upsilon_r^*)$  is also embedded. We will also prove that  $\Upsilon_r^*$  crosses the main diagonal – the fixed point set of  $R$  – exactly once. This information forces the schematic picture of  $\eta_Z \circ E(\partial D_r)$  shown in Figure 6.5.

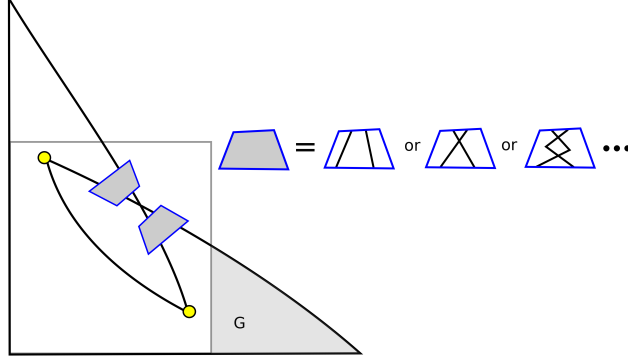


**Figure 6.5:** Schematic picture of  $\eta_Z \circ E(D_5)$ .

Numerically, it seems that the first option occurs, and that the two curves  $\Upsilon_r^*$  and  $R(\Upsilon_r^*)$  intersect exactly once. We did not want to take the trouble to establish this fact, given the already lengthy nature of the paper. In any case, the information above establishes the fact that  $\eta_Z \circ E(\partial D_r)$  winds at most twice around any point in the plane that does not lie in its image. Applying the Disk Lemma to the map  $h = \eta_Z \circ E$  and the disk  $D_r$  we see that  $h$  is at most 2-to-1 on  $D_r$ . But then  $h$  is at most 4-to-1 on  $D_r \cup I(R_r) = S_r^{++}$ . This completes the proof of Projection Estimate 4, modulo the properties of  $\Upsilon_r^*$  and  $\Phi_r^*$ . We now turn to the task of establishing the properties about the topology of this planar loop.

Now we turn to the proof of Projection Estimate 5. It follows from the negative slope of  $\Upsilon_r$  and  $R(\Upsilon_r)$  that any intersection between these two curves lies in the square whose opposite corners are the two cusps. What we mean is that all the “tangles” shown in Figure 6.5 lie inside the lightly shaded square. Hence,  $h$  is injective on the portion of  $D_r$  which maps outside this square. Referring to the Embedding Theorem, the shaded square is bounded by the lines  $x = b_r$  and  $y = b_r$ , where we know that  $b_r < (e^2/2)e^{r/2}$ . The same analysis as done in connection with Equation 29 shows that

$$A_{r,3} + A_{r,4} < K_1 e^{2r/3} + 2I_r,$$

where

$$I_r = \sqrt{2^*} e^{r/2} \int_{x_0}^{(e^2/2)^* e^{r/2}} \frac{dx}{\sqrt{x}} < K_2 e^{3r/4}. \quad (31)$$

These bounds show that  $A_{r,3} + A_{r,4} = 0^* e^r$ . This is Projection Estimate 5.

## 6.6 The Topology of the Boundary

**Lemma 6.4** *For  $r$  sufficiently large, the curve  $\Upsilon_r^* \cup \Phi_r^*$  is embedded.*

**Proof:** Our argument refers to Figure 6.6. Let  $\gamma$  be the portion of  $\Upsilon_r^* \cup \Phi_r^*$  that lies above the (red) horizontal line  $L_1$  through the cusp of  $R(\Upsilon_r^*)$ . This point is the endpoint of  $\Phi_L^*$ .

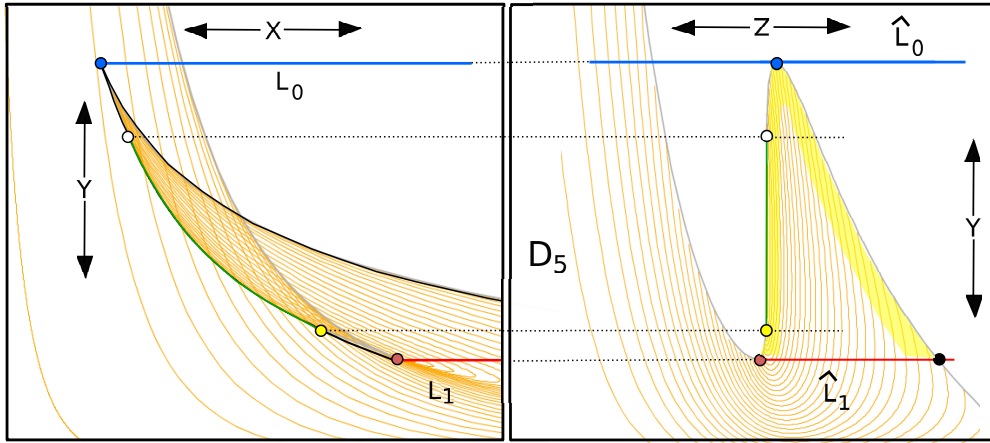


**Figure 6.6:** Projections of the relevant sets.

By the Embedding Theorem,  $\gamma$  has a single cusp, namely the cusp of  $\Upsilon_r$ . Let  $\gamma_1$  and  $\gamma_2$  be the two arcs of  $\gamma$  on either side of this arc. These two arcs have negative slope and no cusps on them. Hence all of  $\gamma$  lies between the horizontal line  $L_0$  through the cusp of  $\Upsilon_r$  and the horizontal line through the cusp of  $R(\Upsilon_r)$ . These are the red and yellow horizontal lines on the left side of Figure 6.6.

Since  $\gamma_1$  and  $\gamma_2$  have negative slope and no cusps, they are each embedded. We just have to see that  $\gamma_1$  cannot intersect  $\gamma_2$ . We will suppose that there is an intersection and derive a contradiction.

The portion of the Sol sphere  $\mathcal{S}_r$  lying in the positive sector is the union of two disks,  $D_r$  and  $R(D_r)$ , where  $R$  is the isometry extending our reflection in the main diagonal of  $\Pi_Z$ , namely  $I(x, y, z) = (y, x, -z)$ . The common boundary of these disks contains a curve  $\hat{\gamma}$  which projects to  $\gamma$ . We have  $\hat{\gamma} = \hat{\gamma}_1 \cup \hat{\gamma}_2$ . On the right side of Figure 6.6, one of these arcs connects the blue vertex to the black vertex, and the other one connects the blue vertex

to the red vertex. The right side of Figure 6.6 shows the projection into the  $YZ$  plane.

Because no plane tangent to  $\mathcal{S}_r$  at an interior point of  $\widehat{\gamma}$  is vertical, each plane of the form  $Y = \text{const.}$  intersects each of  $\widehat{\gamma}_1$  and  $\widehat{\gamma}_2$  exactly once. In particular, this is true to the planes  $\widehat{L}_0$  and  $\widehat{L}_1$  which respectively project to  $L_0$  and  $L_1$  on the left side of Figure 6.6.

One of the two disks  $D_r$  or  $R(D_r)$  has the property that it lies locally between  $\widehat{L}_0$  and  $\widehat{L}_1$  in a neighborhood of  $\widehat{\gamma}$ . We are taking about the yellow highlighted region on the right side of Figure 6.6. The interior of  $D_r$  is transverse to the plane  $\widehat{L}_1$  because  $\eta_Z$  is a local diffeomorphism on the interior of  $D_r$ . But this means that  $D_r \cap \widehat{L}_1$  contains a smooth arc  $\widehat{\beta}$  which connects the endpoint of  $\gamma_1$  to the endpoint of  $\gamma_2$ . Let  $\beta = \eta_Z(\widehat{\beta})$ . We note the following

- $\beta$  is contained in the line  $L_1$ .
- The endpoints of  $\beta$  coincide.
- The interior of  $\beta$  is a regular curve.

These properties are contradictory, because  $\beta$  would have to turn around in  $L_1$  at an interior point, violating the regularity. This contradiction establishes the result that  $\gamma$  is embedded.

It remains to consider the portion of  $\Upsilon_r \cup \Phi_r \cup R(\Upsilon_r^*)$  that lies below the horizontal line  $L_1$  through the cusp of  $R(\Upsilon_r^*)$ . We label so that  $\Phi_r \cup R(\Upsilon_r^*) \subset \gamma_2$ . Given that  $\gamma_2$  has negative slope we see that  $\Phi_r \cup R(\Upsilon_r^*)$  lies entirely above  $L_1$ . But this means that the portion of  $\gamma_1$  below  $L_1$  is disjoint from  $\gamma_2$ . Finally, the portion of  $\gamma_1$  below  $L_1$  is disjoint from the portion of  $\gamma_1$  above  $L_1$  because  $\gamma_1$  is regular and has negative slope. ♠

Define

$$\Upsilon_r^{**} = \Upsilon_r[r, 2r] - \Upsilon_r^*. \tag{32}$$

This is the subset of  $\Upsilon_r[r, 2r]$  that occurs after the cusp. Given our result above, the only self-intersections on the curve  $\eta_Z \circ D(\partial D_r)$  occur where  $\Upsilon_r^{**}$  and  $R(\Upsilon_r^{**})$ . These are analytic arcs of negative slope, and they are permuted by the map  $R$ . Hence, they can only intersect finitely many times, and their intersection pattern must be as in Figure 6.6. This completes the proof of Projection Estimate 4, and hence the Volume Entropy Theorem, modulo the proof of the Embedding Theorem.

The rest of the paper is devoted to proving the Embedding Theorem.

## 7 The Embedding Theorem

### 7.1 The Isochronal Curves

Let  $\underline{\Lambda}_L = (\underline{a}_L, \underline{b}_L)$ , as in §4.3. Let  $E$  be the Riemannian exponential map and let  $\eta_Z$  be projection into the plane  $\Pi_Z$ . We have  $\Upsilon_r = \eta_Z \circ E(Y_r^*)$ , where  $Y_r^*$  is the relevant component of  $Y_r$ .

**Lemma 7.1**  $\Upsilon_r(L) = \underline{\Lambda}_L(r)$ .

**Proof:** Recall that  $S'_r$  is the set of perfect vectors of length  $r$  contained in the positive sector of  $\mathbf{R}^3$ . Define the *positive side* of  $S'_r \cap \Pi_Z$  to be those vectors of the form  $(x, y, 0)$  with  $x > y > 0$ . By definition,

$$\Upsilon_r(L) = \eta_Z \circ E(Y_r^*), \quad (33)$$

where  $Y_r^*$  is the component of the yin yang curve  $Y_r$  which ends in the positive side. The vectors  $V \in Y_r$  are characterized by the property that the differential  $d(\eta_Z \circ E)$  is singular at points of  $Y_r$ .

The kernel of the projection map  $\eta_Z$  is spanned by the vector  $(0, 0, 1)$ . So, the differential  $d(\eta_Z \circ E)$  is singular at  $V$  if and only if  $dE$  maps the tangent plane to  $S'_r$  at  $V$  to a plane which contains the vector  $(1, 0, 0)$ . But then  $dE(N_V)$  is orthogonal to  $(0, 0, 1)$ . Here  $N_V$  is normal to  $S'_r$  at  $V$ . But this means that the third coordinate of  $dE(N_V)$  is 0. Given the connection between the Hamiltonian flow on  $S'_r$  and the geodesics, this situation happens if and only if the flowline associated to  $V$  ends in the plane  $\Pi_Z$ .

In short,  $Y_r$  consists of those small or perfect vectors of length  $r$  whose corresponding flowlines end in  $\Pi_Z$ . But these flowlines are then the initial halves of symmetric flowlines which wind at most twice around their loop level sets. The points in  $Y_r^*$  are the initial halves of symmetric flowlines whose midpoints lie on the positive side of  $S'_r$ . Moreover, these symmetric flowlines wind at most twice around their loop level sets and every amount of winding, so to speak, from 0 times to 2 times, is achieved. So, by definition  $\Upsilon_r = \underline{\Lambda}(r)$ . ♠

We call  $\Upsilon_r$  an *isochronal curve* because it computes all the solutions to the differential equation at the fixed time  $r$ . Figure 7.1 shows part of  $\Upsilon_5$ . The blue curves are the various curves  $\underline{\Lambda}_L[0, L]$ .

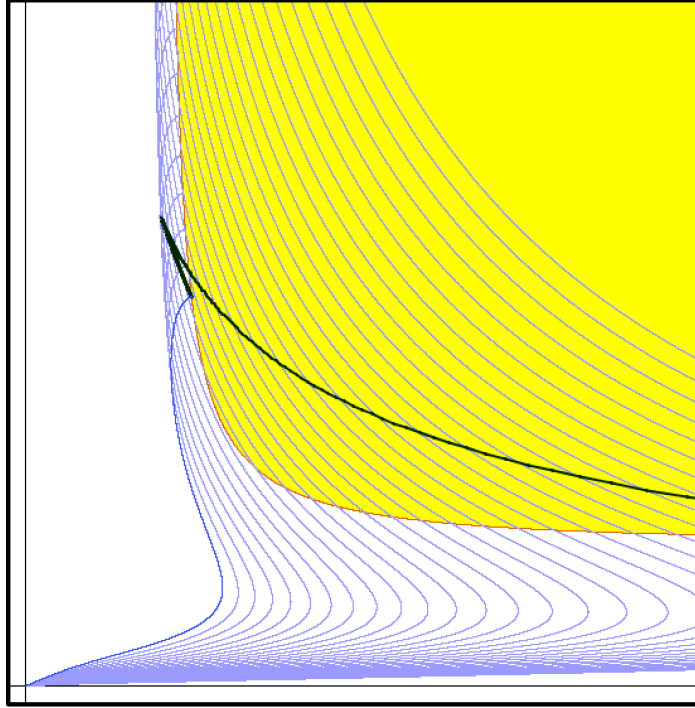


**Figure 7.1:** The  $\underline{\Lambda}_L$  curves and the initial part of  $\Upsilon_5$ .

## 7.2 The Tail End

**Lemma 7.2** *The curve  $\Upsilon_r(2r, \infty)$  is smooth, regular, and embedded.*

**Proof:** The flowline corresponding to the point  $\Upsilon_r(L)$  lies on the loop level set of period  $L$  and flows for time  $r$ . If  $L > 2r$  then the flowline travels less than halfway around the loop level set. Thus, the flowline is the initial half of a small symmetric arc. Let  $S \subset \mathbf{R}^3$  denote the set of vectors corresponding to small symmetric flowlines. The map  $E$  is a diffeomorphism on  $S$ , because  $S$  consists entirely of small vectors. This is part of the Cut Locus Theorem from [CS]. By the Doubling Lemma,

$$\Upsilon_r(2r, \infty) = \frac{1}{2}E(C_r),$$

where  $C_r \subset S$  is a smooth regular curve, obtained by dilating a suitably chosen arc of the yin yang curve by a factor of 2. Since  $E$  is a diffeomorphism on  $S$ , we see that  $\frac{1}{2}E(C_r)$ , is embedded. ♠

### 7.3 The Slope

Let  $x_L$ , etc. be the functions described at the end of §4.3. These functions satisfy the ODE

$$x' = -xz, \quad y' = yz, \quad z' = x^2 - y^2, \quad \underline{a}' = x + az, \quad \underline{b}' = y - bz, \quad (34)$$

with initial conditions

$$x_L(0) > y_L(0) > z_L(0) = \underline{a}_L(0) = \underline{b}_L(0) = 0, \quad (x_L(0), y_L(0), 0) \in \Theta_L. \quad (35)$$

Here  $\Theta_L$  is the loop level set, in the positive sector, having period  $L$ . I am grateful to Matei Coiculescu for help with the following derivation.

**Lemma 7.3**  $\Upsilon_r$  has negative slope away from the cusps.

**Proof:** This proof is a calculation with the ODE. For any relevant function  $f$ , the notation  $\dot{f}$  means  $\partial f / \partial L$ . We compute

$$(\dot{\underline{a}})' = \frac{\partial}{\partial L} \frac{\partial \underline{a}}{\partial t} = \frac{\partial}{\partial L} (x + z\underline{a}) = \dot{x} + \dot{\underline{a}}z + \dot{z}\underline{a}.$$

By the product rule

$$(x\dot{\underline{a}})' = x'\dot{\underline{a}} + x(\dot{\underline{a}})' = -zx\dot{\underline{a}} + x\dot{z} + xz\dot{\underline{a}} + \underline{a}x\dot{z} = x\dot{x} + \underline{a}x\dot{z}.$$

This calculation, and a similar one, show that

$$(x\dot{\underline{a}})' = x\dot{x} + \underline{a}x\dot{z}, \quad (y\dot{\underline{b}})' = y\dot{y} - \underline{b}y\dot{z} \quad (36)$$

Since  $x^2 + y^2 + z^2 \equiv 1$  we have  $x\dot{x} + y\dot{y} + z\dot{z} = 0$ . Adding the Equations in Equation 7.3 and using this relation, we find that

$$(x\dot{\underline{a}} + y\dot{\underline{b}})' = x\dot{x} + y\dot{y} + (ax - by)\dot{z} = x\dot{x} + y\dot{y} + z\dot{z} = 0.$$

Hence  $x\dot{\underline{a}} + y\dot{\underline{b}}$  is a constant function. Since  $\underline{a}(0) = \underline{b}(0) = 0$  for all  $L$  we have  $\dot{\underline{a}}(0) = 0$  and  $\dot{\underline{b}}(0) = 0$ . So, the constant in question is 0. Therefore

$$x\dot{\underline{a}} + y\dot{\underline{b}} = 0 \quad (37)$$

Because  $\Upsilon_r(L) = \underline{\Lambda}_L(r)$ , the velocity of  $\Upsilon_r$  at  $L$  is

$$(\dot{\underline{a}}_L(r), \dot{\underline{b}}_L(r)).$$

This equals  $-x_L(r)/y_L(r)$  by Equation 37. Since  $x, y$  are everywhere positive, the slope of  $\Upsilon_r$  is negative whenever the velocity is nonzero. ♠

## 7.4 The End of Proof

In the next chapter we prove the following result.

**Lemma 7.4 (Monotonicity)** *If  $L$  is sufficiently large then there is some  $t_L \in (L-1, L)$  such that the function  $\underline{b}_L$  is negative on  $[L/2, t_L)$  and positive on  $(t_L, L]$ . Moreover, the function  $L \rightarrow t_L$  is monotone increasing.*

**Corollary 7.5**  $\Upsilon_r[r, 2r]$  *has exactly one cusp.*

**Proof:** The curve  $\Upsilon_r$  has a cusp at  $L$  if and only if its velocity

$$(\dot{a}_L(r), \dot{b}_L(r))$$

vanishes. By Lemma 37, one coordinate of the velocity vanishes if and only if the other one does. So,  $\Upsilon_r$  has a cusp at  $L$  if and only if  $\dot{b}_L(r) = 0$ . Suppose then that  $\Upsilon_r[r, 2r]$  has more than one cusp. Then there are at least two pairs  $(r, L_1)$  and  $(r, L_2)$  such that  $\dot{b}_{L_1}(r) = 0$  and  $\dot{b}_{L_2}(r) = 0$ . This means that  $r = t_{L_1} = t_{L_2}$ . But this contradicts the Monotonicity Lemma. Hence  $\Upsilon_r$  has at most one cusp.

Since the map  $L \rightarrow t_L$  is unbounded, each sufficiently large  $r$  lies in its image. But this means that for sufficiently large  $r$  there is some  $L \in (r, r+1)$  such that  $r = t_L$ . This means that  $\Upsilon_r$  has a cusp at  $L$ . Hence, once  $r$  is sufficiently large,  $\Upsilon_r$  has exactly one cusp. ♠

This completes the proof of the Embedding Theorem, but there is one more remark we want to make. The cusp of  $\Upsilon_r$  occurs at some  $L \in (r, r+1)$ . This explains why, in Figure 7.1, the cusp appears all the way to the left, near the end of  $\Upsilon_5$ .

The next two chapters are devoted to the proof of the Monotonicity Lemma.

## 8 The Vanishing Point

### 8.1 Auxiliary Functions

In this chapter we will prove the first half of the Monotonicity Lemma. That is, we will show that once  $L$  is sufficiently large there is a point  $t_L \in [L-1, L]$  such  $\dot{b}_L$  vanishes at  $t_0$ , and this is the only vanishing point. We sometimes set  $\dot{f} = \partial f / \partial L$  and  $f' = \partial f / \partial t$ . We introduce the following functions.

$$Z = \dot{z}, \quad X = \dot{x}/x, \quad Y = \dot{y}/y, \quad B = \dot{b}/b, \quad (38)$$

Since  $a, b, x, y > 0$  these functions respectively have the same signs as  $\dot{z}, \dot{x}, \dot{y}, \dot{b}$ .

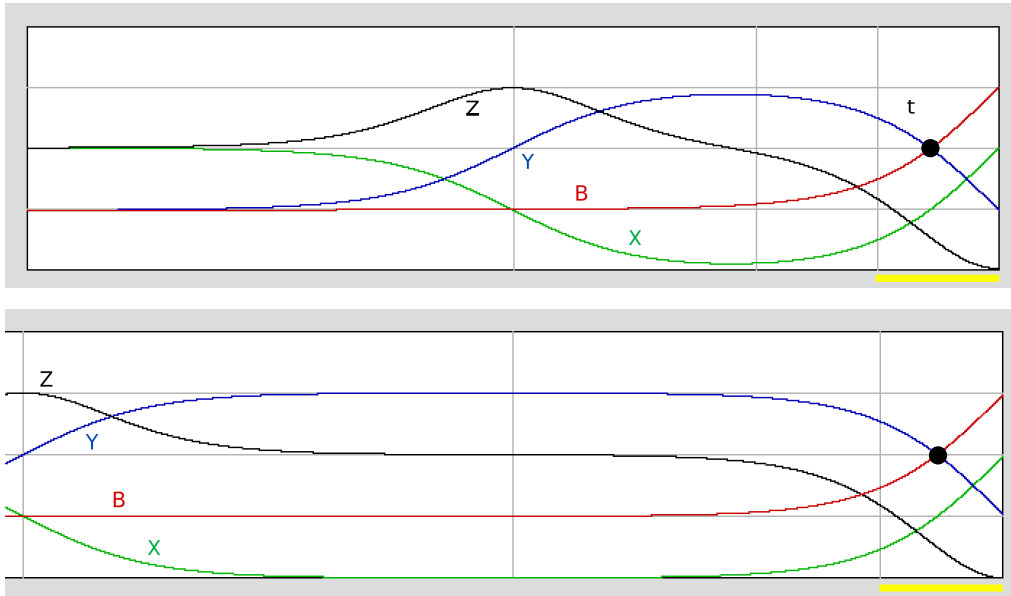


**Figure 8.1:** Numerical plots

The top half of Figure 8.1 shows numerical plots of these functions at  $L = 8$ . The bounding box in the picture is  $[0, 8] \times [-1, 1]$ . The bottom half shows the plot of the functions at the value  $L = 16$ . This time we are just showing the right half of the plot. Notice that in the interval  $[L-1, L]$  the plots line up very nicely. The black dot in both cases is the point  $(t_L, 0)$ . One half of the Monotonicity Lemma establishes that  $t_L$  is uniquely defined. The second half shows that  $t_L$  increases monotonically. The intuition behind the second half of the result is that the pictures in  $[L-1, L]$  stabilize, so that  $t_L = L - s_L$  where  $\partial s_L / \partial L$  is approximately 0 for large  $L$ .

## 8.2 Differentiation Formulas

In this section we derive the following formulas.

1.  $X' = -Z$
2.  $Y' = +Z$
3.  $Z' = -4y^2Y - 2zZ$ .
4.  $B' = \frac{y}{b}(Y - B) - Z$ .
5.  $Z'' = (-2 + 6z^2)Z$ .

(1) From the relation  $x' = -xz$  we get  $(\dot{x})' = -\dot{x}z - \dot{z}x$ . Then we get:

$$X' = \left(\frac{\dot{x}}{x}\right)' = \frac{-\dot{x}z - \dot{z}x}{x} - \frac{\dot{x}x'}{x^2} = -\dot{z} - \frac{\dot{x}z}{x} + \frac{\dot{x}z}{x} = -\dot{z} = -Z$$

(2) From the relation  $y' = yz$  we get  $(\dot{y})' = \dot{y}z + \dot{z}y$ . Then we get:

$$Y' = \left(\frac{\dot{y}}{y}\right)' = \frac{\dot{y}z + \dot{z}y}{y} - \frac{\dot{y}y'}{y^2} = \dot{z} + \frac{\dot{y}z}{y} - \frac{\dot{y}z}{y} = \dot{z} = Z$$

(3) From the relations  $z' = x^2 - y^2$  and  $x^2 = 1 - y^2 - z^2$  we get

$$Z' = 2x\dot{x} + 2y\dot{y} = 2x^2X - 2y^2Y, \quad 2x^2X = -2y^2Y - 2zZ.$$

Substitute the second relation into the first to get the formula above.

(4) Note that  $\frac{\dot{b}}{b} = \dot{b}/b$  because  $\underline{b} = b/2$ . So, we work with  $b$  for ease of notation. From the relation  $b' = 2y - bz$  we get  $(\dot{b})' = 2\dot{y} - \dot{z}b - \dot{z}b$ . Then:

$$\begin{aligned} B' &= \left(\frac{\dot{b}}{b}\right)' = \frac{2\dot{y} - \dot{z}b - \dot{z}b}{b} - \frac{\dot{b}b'}{b^2} = \frac{2\dot{y} - \dot{z}b - \dot{z}b}{b} - \frac{2\dot{b}y - \dot{b}bz}{b^2} = \\ &= \frac{2\dot{y}}{b} - \frac{2\dot{b}y}{b^2} - \dot{z} = \frac{2y}{b}(Y - B) - Z = \frac{y}{\underline{b}}(Y - B) - Z. \end{aligned}$$

(5) We first work out that

$$z'' = -2z + 2z^3. \tag{39}$$

We then compute

$$Z'' = \frac{\partial z''}{\partial L} = \frac{\partial(-2z + 2z^3)}{\partial L} = (-2 + 6z^2)Z.$$

### 8.3 The Formula for B

Here is a formula for  $B$  in terms of the other quantities. Matei Coiculescu found this formula and our derivation follows his ideas.

$$B = \frac{x\underline{a}}{2y\underline{b}}X - \frac{1}{2}Y - \frac{1}{2y\underline{b}}Z. \quad (40)$$

We will work with  $a$  and  $b$  rather than  $\underline{a}$  and  $\underline{b}$  until the end. We have

$$(ax - by)' = 2x^2 - 2y^2 = 2z', \quad a(0) = b(0) = 0.$$

Integrating, we get

$$ax - by = 2z. \quad (41)$$

Given that  $a = 2\underline{a}$  and  $b = 2\underline{b}$ , Equation 37 from the previous chapter is equivalent to:

$$x\dot{a} + y\dot{b} = 0. \quad (42)$$

Differentiating Equation 41 with respect to  $L$ , we have

$$x\dot{a} + a\dot{x} - y\dot{b} - b\dot{y} = 2\dot{z}. \quad (43)$$

Subtracting Equation 43 from Equation 42 we get

$$2y\dot{b} - a\dot{x} + b\dot{y} = -2\dot{z}. \quad (44)$$

Rearranging this, we get

$$\dot{b} = \frac{a\dot{x} - b\dot{y} - 2\dot{z}}{2y}.$$

When we make the substitutions

$$\underline{a} = a/2, \quad \underline{b} = b/2, \quad X = \dot{x}/x, \quad Y = \dot{y}/y, \quad Z = \dot{z},$$

we get Equation 40.

There is a similar formula for the function  $A$ , but we don't need it.

## 8.4 Elliptic Function Calculations

Now we present the two calculations which we will use in the proofs of Lemmas 8.4 and 9.1 below. Define

$$L(y) = 4f(y)\mathcal{K} \circ g(y), \quad (45)$$

where

$$f(y) = \frac{1}{\sqrt{1+2y\sqrt{1-y^2}}} \quad g(y) = \frac{1-2y\sqrt{1-y^2}}{1+2y\sqrt{1-y^2}}. \quad (46)$$

Next define

$$Y_L = \frac{1}{y \times \frac{dL}{dy}}. \quad (47)$$

We use the notation  $f_L \sim g_L$  if  $\lim_{L \rightarrow \infty} f_L/g_L = 1$ .

**Lemma 8.1**  $Y_L \sim -1/2$  and  $\frac{d}{dL}Y_L \sim 0$ .

**Proof:** We compute this in Mathematica, and we get a polynomial expression terms of  $\sqrt{y}$  and  $K = \mathcal{K} \circ g(y)$  and  $E = \mathcal{E} \circ g(y)$ . Taking the series expansions of the coefficients, we find that

$$Y_L = \frac{-1 - 5y + \dots}{\Delta}, \quad \Delta = (2 + 12y + \dots)E + (-4y - 24y^2 + \dots)K. \quad (48)$$

Given that  $g(y) \sim 1 - 4y$ , we see from Equations 8 and 48 that  $Y_L \sim -1/2$ . Next we compute that

$$\frac{\partial}{\partial y}Y_L = \frac{(48y + \dots)E + (-48y + \dots)K}{\Delta^2}. \quad (49)$$

We see from Equations 8 and 49 that  $\frac{\partial}{\partial y}Y_L \sim 0$ . ♠

## 8.5 Asymptotics

If  $f$  and  $g$  are functions of  $L$ , we write  $f \sim g$  if  $f/g \rightarrow 1$  as  $L \rightarrow \infty$ . In this section we prove the following results.

$$(X_L(L/2), Y_L(L/2), Z_L(L/2), B_L(L/2)) \sim (-1/2, 0, 1/2, -1/2),$$

$$(X_L(L), Y_L(L), Z_L(L), B_L(L)) \sim (0, -1/2, -1, 1/2). \quad (50)$$

These various features are already apparent in Figure 8.1. Here we have written e.g.  $X_L$  in place of  $X$  to explicitly indicate how the quantity depends on  $L$ .

**Lemma 8.2**  $Y_L(0) = Y_L(L)$ .

**Proof:** The limits we take for  $Y_L(0)$  and  $Y_L(L)$  respectively are

$$Y_L(0) = \lim_{\epsilon \rightarrow 0} \frac{y_{L+\epsilon}(0) - y_L(0)}{\epsilon y_L(0)}, \quad Y_L(L) = \lim_{\epsilon \rightarrow 0} \frac{y_{L+\epsilon}(L) - y_L(L)}{\epsilon y_L(L)}. \quad (51)$$

Note also that  $y_L(L) = y_L(0)$  and  $y_{L+\epsilon}(L) = y_{L+\epsilon}(\epsilon)$ . Hence

$$Y_L(L) = \lim_{\epsilon \rightarrow 0} \frac{y_{L+\epsilon}(\epsilon) - y_L(0)}{\epsilon y_L(0)}. \quad (52)$$

But the map  $t \rightarrow Y_{L+\epsilon}(t)$  has a local minimum at  $t = 0$  and so  $y_{L+\epsilon}(\epsilon) = y_{L+\epsilon}(0) + O(\epsilon^2)$ . Hence, the limit in Equation 52 equals  $Y_L(0)$ . ♠

**Lemma 8.3**  $X_L(L/2) = Y_L(0)$ .

**Proof:** We have the relations

$$x_L(L/2) = y_L(0), \quad x_{L+\epsilon}(L/2) = y_{L+\epsilon}(\epsilon/2) = y_{L+\epsilon}(0) + O(\epsilon^2).$$

The last equality comes from the fact that the function  $t \rightarrow y_{L+\epsilon}(t)$  has its local minimum at 0. From these relations we have

$$\dot{x}_L(L/2) = \lim_{\epsilon \rightarrow 0} \frac{x_{L+\epsilon}(L/2) - x_L(L/2)}{\epsilon} = \lim_{\epsilon \rightarrow 0} \frac{y_{L+\epsilon}(0) + O(\epsilon^2) - y_L(0)}{\epsilon} = \dot{y}_L(0).$$

The lemma follows from this last equation and from  $x_L(L/2) = y_L(0)$ . ♠

**Lemma 8.4**  $Y_L(0) \sim -1/2$

**Proof:** We set  $y = y_L(0)$ . Using Equation 11 we get an explicit formula for  $L$  in terms of  $y$ . It is given by Equation 45. By the Inverse Function Theorem we have

$$Y_L(0) = \frac{1}{y \times \frac{\partial L}{\partial y}(y)}. \quad (53)$$

By Lemma 8.1, we get  $Y_L(0) \sim -1/2$ . ♠

**Lemma 8.5**  $X_L(0) \sim 0$ .

**Proof:** We differentiate  $x^2 + y^2 + z^2 = 1$  and use  $z_L(0) = 0$  to get

$$x_L^2(0)X_L(0) + y_L^2(0)Y_L(0) = 0. \quad (54)$$

We see that  $X_L(0) \sim 0$  because  $x_L(0) \sim 1$  and  $y_L(0) \sim 0$  and  $Y_L(0) \sim -1/2$  (a finite number). ♠

**Lemma 8.6**  $Z_L(L) \sim -1$  and  $Z_L(L/2) \sim 1/2$ .

**Proof:** We have

$$z_L(L/2) = z(L) = 0, \quad z_{L+\epsilon}(L/2) = z_{L+\epsilon}(\epsilon/2), \quad z_{L+\epsilon}(L) = -z_{L+\epsilon}(\epsilon).$$

Hence

$$-Z_L(L) = \lim_{\epsilon \rightarrow 0} \frac{z_{L+\epsilon}(\epsilon)}{\epsilon} = \lim_{\epsilon \rightarrow 0} \frac{z_{L+\epsilon}(\epsilon) - z_L(\epsilon)}{\epsilon} + \lim_{\epsilon \rightarrow 0} \frac{z_L(\epsilon)}{\epsilon}.$$

The second limit on the right is just  $z'_L(0)$ . The first limit is 0, because

$$z_L(\epsilon) = z'_L(0) + O(\epsilon^2), \quad z_{L+\epsilon}(\epsilon) = z'_{L+\epsilon}(0)\epsilon + O(\epsilon)^2 = (z'_L(0))\epsilon + O(\epsilon)^2.$$

Hence

$$Z_L(L) = -z'_L(0) = y_L^2(0) - x_L^2(0) \sim -1.$$

The proof for  $Z_L(L/2)$  is similar, and indeed  $Z_L(L/2) = -(1/2)Z_L(L)$ . ♠

The rest of the relations for  $X_L$  and  $Y_L$  follow from the ones we have established above, from Lemmas 8.2 and 8.3, and the fact that  $X_L + Y_L$  is a constant function.

**Lemma 8.7**  $B_L(L) \sim 1/2$  and  $B_L(L/2) \sim -1/2$ .

**Proof:** Note that

$$(2\underline{a}_L(L/2), 2\underline{b}_L(L/2), x_L(L/2), y_L(L/2)) = (\underline{b}_L(L), \underline{a}_L(L), y_L(L), x_L(L)).$$

Hence, by the Reciprocity Lemma and the Asymptotic Theorem,

$$2x_L(L/2)\underline{a}_L(L/2) = 2y_L(L/2)\underline{b}_L(L/2) = x_L(L)\underline{a}_L(L) = y_L(L)\underline{b}_L(L) \sim 2.$$

Equation 40 now gives us

$$B_L(L) = \frac{1}{2}X_L(L) - \frac{1}{2}Y_L(L) - \frac{1}{2y_L(L)\underline{b}_L(L)}Z_L(L) \sim$$

$$\frac{1}{2}X_L(L) - \frac{1}{2}Y_L(L) - \frac{1}{4}Z_L(L) \sim 0 + (-1/2)(-1/2) + (-1/4)(-1) = 1/2. \quad (55)$$

The proof for  $B_L(L/2)$  is similar. This completes the proof. ♠

## 8.6 Variation of the Z Coordinate

**Lemma 8.8** Let  $\pi\sqrt{2} < L < M$ . Then  $z_M = z_L$  at most once on  $(0, L)$ .

**Proof:** We already mentioned above that  $z'' = -2z + 2z^3$ . Let  $z_L$  and  $z_M$  be two solutions to this differential equation. Consider the ratio  $\phi = z_M/z_L$ . This quantity is positive on  $(0, L/2]$ . By L'hospital's rule we can continuously extend  $\phi$  to 0, and we have  $\phi(0) > 1$ .

We have

$$\frac{d\phi}{dt} = \frac{W}{z_L^2}, \quad W = z_L z'_M - z_M z'_L, \quad (56)$$

If  $z_L \neq 0$  then  $W$  and  $\phi'$  have the same sign. We compute

$$W' = z_L z''_M - z_M z''_L = 2z_L z_M (z_M^2 - z_L^2). \quad (57)$$

Suppose there is some smallest time  $t \in (0, L/2]$  where  $z_L(t) = z_M(t)$ . Note that  $W' \neq 0$  on  $(0, t)$ . Also,  $W' > 0$  on some small interval  $(0, \epsilon)$  because  $z'_M(0) > z'_L(0)$ . Hence  $W' > 0$  on  $(0, t)$ . Hence  $\phi$  is increasing on  $(0, t)$ . In particular,  $\phi(t) > 1$ . Hence  $z_M(t) > z_L(t)$ , a contradiction.

If there is no time  $t \in (L/2, L)$  where  $z_M(t) = z_L(t)$ , then we are done. Otherwise, let  $t_0$  be the smallest such time. We have  $z_L(t_0) = z_M(t_0) < 0$ . Since  $z_L(t_0 - \epsilon) < z_M(t_0 - \epsilon)$  for small  $\epsilon > 0$ , we have  $z'_M(t_0) \leq z'_L(t_0) < 0$ . Since these two functions are solutions of a second order ODE, namely Equation 39, they cannot have the same initial conditions at  $t_0$ . Hence  $z'_M(t_0) < z'_L(t_0) < 0$ .

Let  $\zeta_L = -z_L$  and  $\zeta_M = -z_M$ . We consider these functions on the interval  $(t_0, L)$ . These are solutions of the same differential equation, with initial conditions  $\zeta_L(t_0) = \zeta_M(t_0)$  and  $0 < \zeta'_L(t_0) < \zeta'_M(t_0)$ . The same argument as above, applied to  $\zeta_L$  and  $\zeta_M$ , shows  $z_L(t) > z_M(t)$  for  $t \in (t_0, L]$ . ♠

**Lemma 8.9 (Z variation)**  $Z_L$  changes sign at most once on  $[0, L]$  and  $Z_L \geq 0$  on  $[0, L/2]$ .

**Proof:** For the first statement, suppose there are 3 points  $t_1, t_2, t_3$  where  $Z_L(t_i)$  for  $i = 1, 2, 3$  alternates sign. But then for  $\epsilon$  sufficiently small, the difference  $z_{L+\epsilon}(t_i) - z_L(t_i)$  also alternates sign for  $i = 1, 2, 3$ . This contradicts Lemma 8.8. So, there at most one  $t_0 \in [0, L]$  where  $Z_L$  changes sign. The second statement follows from the analysis in Lemma 8.8, which showed that  $z_M(t) > z_L(t)$  when  $L < M$  and  $t \in (0, L/2)$ . ♠

## 8.7 Variation of the Y Coordinate

**Lemma 8.10 (Y Variation)** Let  $\delta_0 = 1/7$ . If  $L$  is sufficiently large then:

1.  $|Y_L|, |Z_L| < 5$  on  $[L-1, L]$ .
2.  $Y_L(L) < -\delta_0$ .
3.  $Y'_L < -\delta_0$  on  $[L-1, L]$ .
4.  $Y_L(L-1) > \delta_0$ .
5.  $Y_L > 0$  on  $(L/2, L-1]$ .

**Proof of Statement 1:** Let  $\phi_L(t) = -Z_L(L-1)$ . This function satisfies the differential equation

$$\phi_L(0) = -Z_L(L) \sim 1, \quad \phi'_L(0) = Z'_L(L) \sim 0, \quad \phi''_L(t) = (-2 + 6z_L^2(t))\phi_L(t).$$

For the last equality we used the fact that  $z_L^2(L-t) = z_L^2(t)$ . The solutions to this equation converge in the  $C^\infty$  sense to the solutions of the equation

$$\phi(0) = 1, \quad \phi'(0) = 0, \quad \phi'' = (-2 + 6z^2)\phi. \quad (58)$$

Here  $z$  satisfies  $z'' = -2z + 2z^3$  with initial conditions  $z(0) = 0$  and  $z'(0) = 1$ . Since  $\phi'' \in [-2, 4]\phi$ , and since  $\cos(t\sqrt{2}) > 0$  on  $(0, 1]$ , we have

$$\cos(t\sqrt{2}) \leq \phi(t) \leq \cosh(2t). \quad (59)$$

Since  $\phi_L \rightarrow \phi$  we see that  $|\phi_L| < 2$  once  $L$  is large. Hence  $|Z_L| < 4$  on  $[L-1, 1]$ . Since  $Y_L(L) \sim -1/2$  we have  $|Y_L| < 5$  on  $[L-1, L]$ . ♠

**Proof of Statement 2:** This follows from the fact that  $Y_L(L) \sim -1/2$ .

**Proof of Statement 3:** Let  $\phi_L$  and  $\phi$  be the functions from the previous lemma. For  $t \in [0, 1]$  we have (because  $\phi$  is monotone decreasing)

$$\begin{aligned} Y_L'(L-t) &= Z_L(L-t) = -\phi_L(t) < \epsilon - \phi(t) \leq \\ &\epsilon - \phi(1) \leq \epsilon - \cos(\sqrt{2}) < -1/7 \end{aligned} \quad (60)$$

once  $\epsilon$  is sufficiently small. We can arrange this by taking  $L$  sufficiently large. ♠

**Proof Statement 4:** To estimate  $Y_L(L-1)$  we note that

$$\begin{aligned} Y_L(L-1) &= Y_L(L) - \int_{L-1}^L Z_L dt = Y_L(L) + \int_0^1 \phi_L dt > \\ &-\epsilon - 1/2 + \int_0^1 \phi dt = -\epsilon - 1/2 + \frac{\sin(\sqrt{2})}{\sqrt{2}} > 1/7, \end{aligned} \quad (61)$$

once  $\epsilon$  is sufficiently small. ♠

**Proof Statement 5:** Suppose this is false. Since  $Y_L(L/2) \geq 0$  and  $Y_L'(L/2) = Z_L(L/2) > 0$  we see that  $Y_L$  is somewhere positive on  $(L/2, L-1]$ . Also,  $Y_L(L-1) > 0$  and  $Y_L(L) < 0$ . If  $Y_L = 0$  somewhere else on  $(L/2, L-1]$  then  $Y_L$  switches signs at least 3 times. But then  $Z_L = Y_L'$  switches sign at least twice. This contradicts the Z Variation Corollary. ♠

## 8.8 Variation of the B Coordinate

**Lemma 8.11 (B variation)** *As  $L \rightarrow \infty$ , the function  $Y_L + B_L$  converges to 0 in the  $C^1$  sense.*

**Proof:** We sometimes suppress the dependence on  $L$  in our notation. By Equation 50 we have  $|Y(L) + B(L)| < \epsilon/2$  if  $L$  is sufficiently large. To finish the proof, it suffices to show that  $|B' + Y'| < \epsilon/2$  on  $[L - 1, 1]$  for large  $L$ . Combining our derivative formulas with the preceding two results, we have

$$|B' + Y'| \leq \left| \frac{y}{\underline{b}} \right| \left( \max_{[L-1, L]} |Y| + |B| \right) \leq \frac{10y}{b} < 10y.$$

For the last inequality, we note that  $b(L/2) > 1$  when  $L$  is large and  $b' > 0$  on  $[L/2, L]$ . Hence  $b > 1$  on  $[L - 1, 1]$ . As  $L \rightarrow \infty$  the maximum value of  $y$  on  $[L - 1, L]$  tends to 0. ♠

## 8.9 Uniqueness of the Vanishing Point

In this section we prove the first half of the Monotonicity Theorem. That is, we show that  $\dot{b}_L$  vanishes exactly once on  $(L/2, L)$ . This is the same saying that  $B_L$  vanishes exactly once on  $(L/2, L)$ . Our argument will establish the stronger statement that  $\dot{b}_L$  vanishes somewhere for some  $\lambda \in (L - 1, L)$ . This establishes our assertion we made about the cusp  $\kappa_r$  just after the statement of the Embedding Theorem in

**Lemma 8.12**  *$B_L$  vanishes exactly once in  $[L - 1, L]$ , at an interior point  $t_L$ , and  $B_L(L - 1) < 0$ .*

**Proof:** Combining the Y Variation Lemma and the B Variation Lemma, we get that  $B_L(L - 1) < 0$  and  $B_L(L) > 0$  and  $\dot{B}_L > 0$  on  $[L - 1, L]$ . ♠

Let  $t_1 \in [L/2, L - 1]$  be the smallest value such that  $Z \leq 0$  on  $[t_1, L - 1]$ .

**Lemma 8.13**  *$B_L < 0$  on  $[t_1, L - 1]$ .*

**Proof:** Since  $Z_L(L-1) < 0$  we know that  $t_1 \in [L/2, L-1)$ . We introduce the function  $\phi(t) = -B_L(L-1-t)$ . We have  $\phi(0) > 0$  and  $\phi'(t) = B'_L(L-1-t)$ . Hence

$$\frac{\partial \phi}{\partial t} = \frac{y_L(L-1-t)}{\underline{b}_L(L-1-t)} \times \left( Y_L(L-1-t) + \phi(t) \right) - 2Z_L(L-1-t).$$

By the Y Variation Lemma and the definition of  $t_1$  we have  $\phi' = \mu_1\phi + \mu_2$  where  $\mu_1$  and  $\mu_2$  are non-negative functions on  $[0, L-1-t_1]$ . Since  $\phi(0) > 0$  we have  $\phi > 0$  on  $[0, L-1-t_1]$ . Hence  $B_L < 0$  on  $[t_1, L-1]$ . ♠

If  $t_1 = L/2$  this next lemma is vacuous.

**Lemma 8.14**  $B_L < 0$  on  $(L/2, t_1)$ .

**Proof:** Here is Equation 40 again:

$$B = \frac{x\underline{a}}{2y\underline{b}}X - \frac{1}{2}Y - \frac{1}{2y\underline{b}}Z.$$

Our result here follows from Equation 40 and these inequalities on  $[L/2, t_1)$ :

- The quantities  $x_L, y_L, \underline{a}_L, \underline{a}_L$  are all positive.
- Since  $X_L(L/2) \leq 0$  and  $X'_L = -Z_L \leq 0$  on  $(L/2, t_1)$ , we have  $X_L \leq 0$ .
- By the Y Variation Lemma,  $Y_L > 0$ .
- Since  $Z_L$  changes sign only at  $t_1$ , and  $Z_L(L) < 0$ , we have  $Z_L \geq 0$ .

This completes the proof. ♠

## 8.10 Bounds on the Cusp

Now we prove the claim in the Monotonicity Theorem concerning the location of the cusp

$$\kappa_r = (a_r, b_r, c_r).$$

We use the same notation established at the beginning of §5. We treat the bounds one at a time.

**Lemma 8.15**  $a_r < 2^*$ .

**Proof:** Let  $\Upsilon_r$  be the isochronal curve. Let  $\kappa'_r = (a'_r, b'_r, 0)$  be the upper endpoint of the arc  $P$ . We know from the Asymptotic Theorem and from Lemma 2.1 that  $a'_r < 2^*$ . The portion of  $\Upsilon_r$  connecting  $\kappa_r$  to  $\kappa'_r$  has negative slope. Hence  $a_r < a'_r < 2^*$ . ♠

**Lemma 8.16**  $b_r < (e^2/2)^* e^{r/2}$ .

**Proof:** By Lemma 8.12, we have

$$\kappa_r \in \Upsilon_\lambda(L) \tag{62}$$

for some  $\lambda \in (L - 1, L)$ . Let  $f_{r,\lambda}$  be the flowline corresponding to  $\kappa_r$ . From what we have just said, the flowline  $f_{r,\lambda}$  corresponding to  $\kappa_r$  lies in the loop level set of period  $\lambda$ , winds almost all the way around its loop level set, and ends in the plane  $Z = 0$ .

Consider the following perfect flowlines:

- $f_\lambda$  is the perfect symmetric flowline which has the same ending point as  $f_{r,\lambda}$ . Let  $\Lambda_f \in \Pi_Z$  be the point corresponding to  $f_\lambda$ .
- $g_\lambda$  is the perfect symmetric flowline which has the same initial point as  $f_{r,\lambda}$ . Let  $\Lambda_g \in \Pi_Z$  be the point corresponding to  $g_\lambda$ .

By Lemma 2.1 we have

$$\Lambda_f = (\alpha_f, \beta_f, 0), \quad \beta_f < (1/2)^* e^{\lambda/2}. \tag{63}$$

Given the properties of concatenation, we have some element  $h \in \text{Sol}$  whose third coordinate lies in  $(-1, 1)$ , such that

$$(\alpha_g, \beta_g, 0) = \Lambda_g = h * \Lambda_f * h^{-1}. \tag{64}$$

Conjugation by an element whose third coordinate lies in  $(-1, 1)$  changes the first and second coordinates by a factor of at most  $e$ . Hence

$$\beta_g < (e/2)^* e^{\lambda/2} < (e^2/2)^* e^{r/2}. \tag{65}$$

The flowline  $g_\lambda$  is the extension of  $f_{r,\lambda}$  by at most 1 unit of flow. Hence the distance from  $\Lambda_g$  to  $\kappa_r$  is less than 1 unit. Moreover, both points lie in the slab  $|Z| < 1$ , where the metric is boundedly close to Euclidean. Hence, we get the same bound on  $b_r$  as we got on  $\beta_g$ . Hence  $b_r < (e^2/2)^* e^{r/2}$ . The universally small additive constant is just absorbed into the bound. ♠

## 9 Monotonicity of the Vanishing Point

### 9.1 The Proof Modulo Asymptotics

We know there is a unique  $t_L \in (L-1, L)$  where  $\dot{b}_L$  vanishes. In this chapter we show that  $t_L$  is monotone increasing. Let

$$\beta_L(t) = -B_L(L-t). \quad (66)$$

There is a unique  $s_L \in (0, 1)$  such that  $\beta_L(s_L) = 0$ . In fact,  $t_L = L - s_L$ . Since  $\dot{t}_L = 1 - \dot{s}_L$ , it suffices to show  $|\dot{s}_L| < 1$  for large  $L$ . We show  $\dot{s}_L \sim 0$ . That is,  $\lim_{L \rightarrow \infty}(\dot{s}_L) = 0$ . Define

$$\delta(t) = \frac{y(L-t)}{b(L-t)}, \quad \phi(t) = Y(L-t), \quad \zeta(t) = Z(L-t). \quad (67)$$

Since  $\beta'(t) = B'(L-t)$ , we have

$$\beta' = \delta(\phi - \beta) - \zeta, \quad (\dot{\beta})' = \dot{\delta}(\phi - \beta) + \delta(\dot{\phi} - \dot{\beta}) - \dot{\zeta}. \quad (68)$$

The second equation comes from differentiating the first with respect to  $L$ .

Let  $\|f\|$  denote the sup of  $f$  on  $[0, 1]$ . We will establish the following estimates below.

$$\|\delta\|, \|\dot{\delta}\|, \|\dot{\phi}\|, \|\dot{\zeta}\|, \dot{\beta}(0) \sim 0. \quad (69)$$

We also know from the Y Variation Lemma that  $\|\phi\|, \|\zeta\| < 5$ . Hence

$$(\dot{\beta})' = \epsilon_1 \dot{\beta} + \epsilon_2, \quad (70)$$

where  $\epsilon_1$  and  $\epsilon_2$  are functions such that  $\|\epsilon_1\|, \|\epsilon_2\| \sim 0$ . Given our initial condition  $\dot{\beta}(0) \sim 0$ , a standard comparison argument now says that  $\|\dot{\beta}\| \sim 0$ .

By definition

$$\beta_L(s_L) = 0. \quad (71)$$

Using implicit differentiation, we see that

$$|\dot{s}_L| = \left| \frac{\dot{\beta}(s_L)}{\beta'(s_L)} \right| < 8|\dot{\beta}(s_L)| \sim 0. \quad (72)$$

The last inequality comes from the fact that  $|\beta'| > 1/8$  on  $[L-1, L]$  once  $L$  is large enough. This proves the Monotonicity Lemma, modulo Equation 69.

## 9.2 The Asymptotics

We say that a function  $f$  of  $L$  is *tame* if  $df/dL \sim 0$ . If  $f$  is analytic (i.e. not contrived in an artificial way) and  $f \sim \text{const.}$  one might expect  $f$  to be tame. We verify that this is the case for a number of quantities we have studied in the previous chapter. We also point out, when relevant, how the given quantity relates to the functions  $\beta, \delta, \phi, \zeta$  introduced above.

**Lemma 9.1**  $Y_L(L)$  is tame. Hence  $\dot{\phi}(0) \sim 0$ .

**Proof:** Since  $Y_L(0) = Y_L(L)$ , it suffices to prove that  $Y_L(0)$  is tame. Lemma 8.1 tells us that

$$\frac{d}{dy}Y_L(0) \sim 0, \quad (73)$$

where  $y = y_L(0)$ . But, since  $Y_L(0)$  is asymptotic to a finite number, and  $y_L(0) \sim 0$ , we have  $\frac{dy}{dL} \sim 0$ . Therefore, *a fortiori* we have  $\frac{d}{dL}Y_L(0) \sim 0$ . ♠

**Lemma 9.2**  $X_L(L)$  is tame.

**Proof:** Since  $X_L(0) = X_L(L)$ , it suffices to prove that  $X_L(0)$  is tame. Differentiating Equation 54 with respect to  $L$ , we get

$$2x_L^2(0)X_L^2(0) + x_L^2(0)\left(\frac{d}{dL}X_L(0)\right) + 2y_L^2(0)Y_L^2(0) + y_L^2\left(\frac{d}{dL}Y_L(0)\right) = 0. \quad (74)$$

Given that  $x_L(0) \sim 1$  and  $y_L(0) \sim 0$  and  $Y_L(0) \sim -1/2$  and that  $Y_L(0)$  is tame, we see that  $X_L(0)$  is also tame. ♠

**Lemma 9.3**  $Z_L(L)$  is tame. Hence  $\dot{\zeta}(0) \sim 0$ .

**Proof:** We have

$$\frac{d}{dL}Z_L(L) = \frac{d}{dL}(y_L^2(0) - x_L(0)^2) = y_L^2(0)Y_L(0) - x_L^2(0)X_L(0) \sim 0.$$

The last equation comes from the fact that all quantities in the last expression are asymptotic to finite numbers and  $y_L(0) \sim 0$  and  $X_L(0) \sim 0$ . ♠

**Lemma 9.4**  $Z'_L(L)$  is tame. Hence  $(\dot{\zeta})'(0) \sim 0$ .

**Proof:** Since  $z_L(L) = 0$  we have

$$Z'_L(L) = -4y_L^2(L)Y_L(L). \quad (75)$$

Differentiating Equation 75 with respect to  $L$  and using the product rule, as above, we see that  $\frac{d}{dL}Z'_L \sim 0$ . ♠

**Lemma 9.5**  $y_L(L)\underline{b}_L(L)$  is tame.

**Proof:** We begin by proving an estimate that will come in at the end of the proof. We claim that

$$\max_{[0, L/4]} |Y_L| < 1. \quad (76)$$

To see this, note that  $Y'_L = Z_L$ . We also know that  $Z_L \geq 0$  on  $[0, L/2]$ . Hence  $Y_L$  is monotone increasing on  $[0, L/2]$  and  $Y_L(L/2) \sim 1/2$ . This establishes Equation 76.

By Lemma 5.1, we see that

$$y_L(L)b_L(L) = 2z_L(L/4) + 2\phi_L, \quad \phi_L = \int_0^{L/4} y_L^2 dt. \quad (77)$$

We deal with these terms one at a time. Referring to Equation 11 we have  $z_L(L/4) = \sqrt{1 - 2\alpha_L^2}$ . Here  $\alpha_L \sim 0$ . This leads to  $\frac{d}{d\alpha}(Z_L(L/4)) \sim 0$ . A calculation like the one done in Lemma 8.4 shows that  $|dL_\alpha/d\alpha| \sim \infty$ . Hence  $d\alpha_L/dL \sim 0$ . But then, by the chain rule,  $\frac{d}{dL}z_L(L/4) \sim 0$ .

We have

$$\frac{d\phi_L}{dL} = \int_0^{L/4} \frac{\partial}{\partial L}(y_L)^2 dt + \frac{1}{4}y_L(L/4). \quad (78)$$

Referring to Equation 11 we have  $y_L(L/4) = \alpha$ . So, the same argument as for  $Z_L(L/4)$  now shows that  $\frac{d}{dL}y_L(L/4) \sim 0$ . Finally, we have

$$\int_0^{L/4} \frac{\partial}{\partial L}(y_L)^2 dt = 2 \int_0^{L/4} y_L^2 Y_L dt \leq^* 2 \int_0^{L/4} y_L^2 \sim 0.$$

The starred inequality comes from Equation 76. The final asymptotic result comes from the proof of Lemma 5.1. ♠

All of the asymptotic results we have obtained so far feed into one final one.

**Lemma 9.6**  $B_L(L)$  is tame. Hence  $\dot{\beta}(0) \sim 0$ .

**Proof:** As in Lemma 8.7 have

$$B_L(L) = X_L(L) - \frac{1}{2}Y_L(L) - \frac{1}{y_L(L)\underline{b}_L(L)}Z_L(L) \sim$$

$$X_L(L) - \frac{1}{2}Y_L(L) - \frac{1}{4}Z_L(L) \sim 0 + (-1/2)(-1/2) + (-1/4)(-1) = 1/2. \quad (79)$$

We know that

$$X_L(L), Y_L(L), Z_L(L), y_L(L)\underline{b}_L(L)$$

are all tame. Also, we know that

$$y_L(L)\underline{b}_L(L) \sim 2,$$

by the Asymptotic Theorem. Using all this information, and the product and quotient rules for differentiation, we see that  $B_L(L)$  is tame. ♠

**Lemma 9.7**  $\|Z\| \sim 0$ .

**Proof:** Our notation here is a bit funny. We mean to restrict our function  $Z_L$  to the interval  $[0, 1]$  and take its maximum. We have  $Z(0) \sim 0$  and  $|Z''| \leq 4|Z|$ . Since  $Z > 0$  on  $(0, 1]$ , the same kind of comparison argument used in the proof of the Y Variation Lemma now shows that  $\max_{[0,1]} |Z| \leq Z(0) \cosh(2) \sim 0$ . ♠

Now we establish the remaining estimates from §9.1

**Lemma 9.8**  $\|\delta\| \sim 0$  and  $\|\dot{\delta}\| \sim 0$ .

**Proof:** The argument in the proof of the B Variation Lemma shows, incidentally, that  $\|\delta\| \sim 0$ . Using our derivative formulas, we have

$$\dot{\delta}(t) = (Y(L-t) - B(L-t))\delta(t).$$

Combining the Y Variation Lemma and the B Variation Lemma we see that  $|B|, |Y| < 6$  on  $[L-1, L]$  for large  $L$ . Hence  $\|\dot{\delta}\| < 12\|\delta\| \sim 0$ . ♠

**Lemma 9.9**  $\|\dot{\zeta}\| \sim 0$ .

**Proof:** Define  $\eta = \dot{\zeta}$ . From the differential equation for  $Z''$  and the fact that  $z_{L-t} = z_t$  we get  $\zeta''(t) = (-2 + 6z^2(t))\zeta$ . Differentiating with respect to  $L$  and using the fact that the mixed partials commute, we see that

$$\dot{\zeta}''(t) = (-2 + 6z^2(t))\dot{\zeta}(t) + 12Z(t)z^2(t)\zeta(t).$$

The first term on the right lies in  $[-4, 4]\dot{\zeta}(t)$ . The second term is at most

$$12\|Z\| \max_{[L-1, L]} |Z| < 60\|Z\| \sim 0.$$

Here we have used Statement 1 of the Y Variation Lemma and also the bound from Lemma 9.7. Putting these estimates together, we get

$$|\dot{\zeta}''| \leq 4|\dot{\zeta}(t)| + \epsilon, \tag{80}$$

where  $\epsilon \sim 0$ . We have already seen that  $\dot{\zeta}(0) \sim 0$  and  $(\dot{\zeta})'(0) \sim 0$ . The same kind of comparison argument as above now give us the desired bound on  $\dot{\zeta}$ . ♠

**Lemma 9.10**  $\|\dot{\phi}\| \sim 0$ .

**Proof:** We have  $\phi' = -\zeta$ . Differentiating with respect to  $L$  we get

$$(\dot{\phi})' = -\dot{\zeta}.$$

We also have  $\dot{\phi}(0) \sim 0$ . We now integrate the bound on  $\|\dot{\zeta}\|$  to get the bound on  $\|\dot{\phi}\|$ . ♠

With these bounds, we complete the proof of the Monotonicity Lemma.

## 10 References

- [A] V. I. Arnold, *Sur la géométrie différentielle des groupes de Lie de dimension infinie et ses applications à l'hydrodynamique des fluides parfaits*. Ann. Inst. Fourier Grenoble, (1966).
- [AK] V. I. Arnold and B. Khesin, *Topological Methods in Hydrodynamics*, Applied Mathematical Sciences, Volume 125, Springer (1998)
- [B] N. Brady, *Sol Geometry Groups are not Asynchronously Automatic*, Proceedings of the L.M.S., 2016 vol 83, issue 1 pp 93-119
- [BB] J. M. Borwein and P. B. Borwein, *Pi and the AGM*, Monographies et Études de la Société Mathématique du Canada, John Wiley and Sons, Toronto (1987)
- [BS] A. Bölcskei and B. Szilágyi, *Frenet Formulas and Geodesics in Sol Geometry*, Beitrage Algebra Geom. 48, no. 2, 411-421, (2007).
- [BT], A. V. Bolsinov and I. A. Taimanov, *Integrable geodesic flow with positive topological entropy*, Invent. Math. **140**, 639-650 (2000)
- [CMST] R. Coulon, E. A. Matsumoto, H. Segerman, S. Trettel, *Noneuclidean virtual reality IV: Sol*, math arXiv 2002.00513 (2020)
- [CS] M. P. Coiculescu and R. E. Schwartz, *The Spheres of Sol*, submitted preprint, 2020
- [EFW] D. Fisher, A. Eskin, K. Whyte, *Coarse differentiation of quasi-isometries II: rigidity for Sol and Lamplighter groups*, Annals of Mathematics 176, no. 1 (2012) pp 221-260
- [G], M. Grayson, *Geometry and Growth in Three Dimensions*, Ph.D. Thesis, Princeton University (1983).
- [K] S. Kim, *The ideal boundary of the Sol group*, J. Math Kyoto Univ 45-2 (2005) pp 257-263

[**KN**] S. Kobayashi and K. Nomizu, *Foundations of Differential Geometry, Volume 2*, Wiley Classics Library, 1969.

[**LM**] R. López and M. I. Muntanu, *Surfaces with constant curvature in Sol geometry*, Differential Geometry and its applications (2011)

[**S**] R. E. Schwartz, *Java Program for Sol*, download (in 2019) from <http://www.math.brown.edu/~res/Java/SOL.tar>

[**T**] M. Troyanov, *L'horizon de SOL*, Exposition. Math. 16, no. 5, 441-479, (1998).

[**Th**] W. P. Thurston, *The Geometry and Topology of Three Manifolds*, Princeton University Notes (1978). (See <http://library.msri.org/books/gt3m/PDF/Thurston-gt3m.pdf> for an updated online version.)

[**W**] S. Wolfram, *The Mathematica Book, 4th Edition*, Wolfram Media and Cambridge University Press (1999).